

OPTICAL SUBSTRUCTURES IN 48 GALAXY CLUSTERS: NEW INSIGHTS FROM A MULTI-SCALE ANALYSIS

M. GIRARDI^{1,2}, E. ESCALERA^{1,2,3}, D. FADDA^{1,2}, G. GIURICIN^{1,2}, F. MARDIROSSIAN^{1,2,4} AND M. MEZZETTI^{1,2}

¹Dipartimento di Astronomia, Università degli Studi di Trieste,

²SISSA, via Beirut 4, 34013 - Trieste, Italy

³Observatoire de Marseille, Place Le Verrier, F-13248, Marseille, Cédex 4, France

⁴Osservatorio Astronomico di Trieste, Italy

E-mail: girardi@sissa.it; escalera@obmara.cnrs-mrs.fr; giuricin@sissa.it; fadda@sissa.it; mezzetti@sissa.it

ABSTRACT

We analyze the presence of substructures in a set of 48 galaxy clusters, by using galaxy positions and redshifts. The data are taken from literature sources, with the addition of some new data provided by recent observations of galaxy clusters.

We use a multi-scale analysis which couples kinematical estimators with the wavelet transform. With respect to previous works, we introduce three new kinematical estimators. These estimators parameterize the departures of the local means and/or local dispersions of the measured radial velocities with respect to their global values for the environment.

We classify the analyzed clusters as unimodal, bimodal and complex systems. We find that $\sim 14\%$ of our clusters are strongly substructured (i.e. they are bimodal or complex) and that $\sim 24\%$ of the remaining unimodal clusters contain substructures at small scales. Thus, in substantial agreement with previous studies, about one third of clusters show substructures.

We find that the presence of substructures in unimodal clusters does not affect the estimates of both velocity dispersions and virial masses. Moreover, the galaxy velocity dispersion is generally in good agreement with the X-ray temperature, according to the expectations of the standard isothermal model for galaxy clusters. These facts suggest that unimodal clusters, which are the most frequent cases in the nearby Universe, are not too far from a status of dynamical equilibrium.

On the contrary, the estimates of velocity dispersions and masses for some bimodal or complex clusters strongly depend on whether they are treated as single systems or as sums of different clumps. In these cases the X-ray temperature and the velocity dispersion may be very different.

Subject headings: galaxies: clusters: general – galaxies: clustering – cosmology: observations – methods: data analysis

1 INTRODUCTION

The recent literature has provided firm evidence of the presence of substructures in galaxy clusters (see West 1994, and references therein). Indeed, when the amount of data grows and the techniques of analysis are improved, the clusters show more and more substructures (see, e.g., recent results on the Coma cluster by Biviano et al. 1996).

The effect of substructures on cluster kinematics and dynamics is widely studied in the literature. The presence of substructures could make the galaxy velocity distributions deviate from Gaussian ones (Bird & Beers 1993; Zabludoff, Franx, & Geller 1993). Beers & Tonry (1986) suggested that the constant density cores of clusters are actually due to the presence of central substructures. Substructures could also cause the observed significant velocity offsets of cD galaxies with respect to other cluster members (Sharples, Ellis, & Gray 1988; Hill et al. 1988).

The presence of substructures could lead to over- or underestimates of the galaxy velocity dispersions (e.g. Fitchett 1988), to overestimates of the cluster mass (Pinkney et al. 1996), and could also modify the velocity dispersion profile in the central cluster region (Fitchett & Webster 1987). In particular, these effects are suggested as caus-

ing the disagreement between the observed velocity dispersion of galaxies and X-ray temperature of hot gas (Edge & Stewart 1991b). On the other hand, collisions of subclusters can enhance the X-ray temperature (e.g. Briel & Henry 1994; Zabludoff & Zaritsky 1995).

Also numerical simulations show that both galaxy velocity dispersion and gas temperature increase during a phase of cluster merging (see e.g. Evrard 1990; Schindler & Boehringer 1993; Schindler & Mueller 1993; Roettiger, Burns, & Loken 1993; Burns et al. 1995). Therefore, in cases of strong substructures, e.g. close bimodal clusters, both galaxy velocity dispersion and gas X-ray temperature may be bad measures of the cluster potential since the cluster may be very far from a status of dynamical equilibrium.

The situation is less clear for clusters with small substructures, which are the most frequent cases and thus the most important ones in statistical analyses, e.g. in the observational distribution function of cluster masses, since, to evaluate cluster masses, a status of dynamical equilibrium is generally assumed (e.g. Bahcall & Cen 1993; Biviano et al. 1993). Recent results from numerical simulations suggest that, on average, clusters could be approximately in dynamical equilibrium within a central region

(e.g. Tormen, Bouchet, & White 1996). From the observational point of view, partially contradictory conclusions are reached by two recent works - based on large cluster samples - which look for substructures by using galaxy positions and redshifts (Escalera et al. 1994, hereafter E94; Bird 1995, hereafter B95).

By examining 16 clusters, E94 found that the sum of virial masses of gravitationally bounded internal structures is generally close to the total virial mass of the main cluster. On the contrary, B95 found that the correction for the presence of substructures appreciably affects the masses of 25 clusters with a dominant galaxy, the effect being mainly due to a reduction of the mean galaxy separation. However, B95 found that the correction for substructures is not significant if the cluster mass is computed within the virialization radius (see B95) rather than within an Abell radius. Both works agree in claiming that the velocity dispersion is not strongly biased by the presence of substructures.

Another critical question concerns the survival time of a substructure within the cluster (see e.g. Gonzales-Casado, Mamon, & Salvador-Solé 1994), which is essential for constraining the critical density of the Universe by using the frequency of substructures (Lacey & Cole 1993; Ueda et al. 1995). The poor knowledge of the frequency, nature and origin of substructures makes the problem more difficult.

The availability of a large amount of new redshifts for cluster galaxies (e.g. Katgert et al. 1996) allows us to better investigate cluster structures. The redshift information greatly alleviates the problems induced by the presence of cluster interlopers and/or cluster overlapping, problems which are always present in two-dimensional analyses. With respect to studies based on X-ray data, an optical analysis may have the advantages of allowing a three-dimensional analysis, of identifying the galaxies belonging to different subclumps, and of investigating the outer cluster regions of low X-ray surface brightness. On the other hand, because of the still small number of measured galaxy redshifts we need very refined techniques for substructure analyses.

For instance, a suitable technique is wavelet analysis, which can be performed on optical, X-ray (Slezak et al. 1994), and radio data (Grebenev et al. 1995). The wavelet analysis was first applied to astrophysics as a two-dimensional technique by Slezak et al. (1990). Subsequently, Escalera & Mazure (1992) improved the technique by coupling it to redshift information. In this paper we describe a further improvement in order to better detect substructures in galaxy clusters.

The identification of galaxies involved in structures allows us both to collect information concerning the substructures themselves and to analyze their kinematical and dynamical effect on clusters. The difficulty in these analyses arises from the possible presence, also in virialized systems, of velocity anisotropies in galaxy orbits, which makes it difficult to deproject l.o.s. (i.e. line of sight)

galaxy velocities. These problems are taken into account in our analyses, as well as in our substructure detection.

In § 2 we describe the main dataset used in this work. § 3 is a description of our method. In § 4 we display the main results of the structure identification for the 48 clusters with respective kinematical analysis. The results for each cluster are discussed in the appendix. Then, in § 5, we attempt a classification of typical cluster morphologies and present our general results and discussions regarding the kinematical and dynamical effect of the substructures. In § 6 we draw our conclusions.

Throughout, all errors are at the 68% confidence level (hereafter c.l.), while the Hubble constant is $100 h^{-1} Mpc^{-1} km s^{-1}$.

2 THE DATA SAMPLE

We apply our procedure to a set of 48 galaxy clusters, whose data are taken mainly from literature sources and also from the recent *ESO Nearby Abell Clusters Survey (ENACS)*¹, described in Katgert et al. (1996). The clusters considered are Abell clusters except for the poor cluster MKW3S, which belongs to the cluster field of A2063.

Only well-sampled clusters with a good level of completeness in magnitude are suitable for detecting substructures. In fact, cluster regions which are oversampled with respect to the rest of the cluster could produce artifacts which are not real substructures. Also a galaxy sample randomly extracted from a magnitude-complete sample is adequate to the study of substructures, although in this case there is an obvious loss of information.

Here we considered only galaxy samples which nominally have the above characteristics. If necessary, we extracted from the whole data sample a magnitude-complete one, according to the information given by the authors. When more than one redshift source is used, we checked that a certain level of completeness is still conserved. Out of the 48 clusters, ten include some data from ENACS in order to improve the completeness in velocities (see Table 1); of these, A151 and A3128 have almost exclusively ENACS data. We accept clusters with a minimum level of magnitude completeness of 80%. For some clusters, for which we do not have full information on magnitude, the completeness level is considered acceptable by the authors. In four cases (A539, A1060, A2670 and A3526), we considered also an alternative initial sample, indicated by an asterisk in Table 1, with a lower completeness level or a smaller extension. These alternative samples are considered less useful for structure analysis and are used only to investigate or confirm particular effects. In all cases we refer to the authors for the characteristics of completeness limits.

To fulfill the completeness requirements, information is given throughout the whole field down to a limiting magnitude, and therefore the foreground and background objects are systematically included.

¹Concise information on the ENAC Survey is available on the WWW at <http://www.eso.org/educnpublicns/pr-05-96.html>

TABLE 1
THE DATA SAMPLE

Cluster Name (1)	N_{field} (2)	RS type (3)	Velocities Ref. (4)	Magnitudes Ref. (5)	T_X Ref. (6)	X-ray centers Ref. (7)
A0085.....	185	cD	3,38	...	12	20
A0119.....	139	C	21,23	21,23	12	1
A0151.....	142	cD	21,49	16,21	18*	18
A0193.....	65	cD	31	...	12	19
A0194.....	200	L	9	9	34	7
A0262.....	88	C	25,28,42	...	12	20
A0399.....	227	cD	31	...	12	1
A0401.....	227	cD	31	...	12	1
A0426.....	128	L	35	35,63	12	20
A0539 (A0539*)...	189(153)	F	45	43,64	12	1
A0548.....	401	(F)	17,21	17,21	13	13
A0754.....	89	cD	17	17	12	63
A1060 (A1060*)...	101(144)	C	52,53	52,53	33	20
A1146.....	84	cD	58	...	57*	46
A1185.....	77	C	3	...	12	4
A1367.....	68	F	15,24,26,59	64	12	29
A1631.....	90	C	17	17	18*	18
A1644.....	102	cD	17	17	12	20
A1736.....	104	I	17	17	12	6
A1795.....	98	cD	31	...	12	19
A1809.....	69	cD	21,31	21	18*	18
A1983.....	100	F	17	17	18*	18
A2052.....	60	cD	21,38,50	21,64	12	1
A2063.....	141	cD	3,31	16	12	4
A2107.....	75	cD	44	...	12	41
A2124.....	67	cD	31	...	18*	51
A2151.....	106	F	17	17	12	51
A2197.....	89	L	27	64	30*	51
A2199.....	89	cD	27	17	12	51
A2634.....	403	cD	5,8,32,48,54,62	5,8,32,62	12	53
A2666.....	403	cD	5,8,32,48,54,62	5,8,32,62	30*	29
A2670 (A2670*)...	122(88)	cD	55	55	12	4
A2717.....	81	cD ^b	10,21	11,21	18*	18
A2721.....	104	cD	10,58	11	18*	18
A2877.....	110	C	38	16	12	29
A3128.....	222	C	10,21	11,21	18*	18
A3266.....	172	cD	58	...	12	29
A3376.....	84	L	17	17	18*	18
A3391.....	284	cD ^c	58	...	12	29
A3395.....	284	F	58	...	12	29
A3526 (A3526*)...	123(105)	F	14,36	14,36	12	20
A3558.....	551	cD ^b	2,21,39,52,58	2,21,39	12	6
A3562.....	551	...	2,21,39,52,58	2,21,39	12	19
A3667.....	177	L ^a	21,56	21,56	12	47
A3716.....	106	F	10,17	17	18*	18
A3888.....	98	C	58	...	60	29
A4038.....	51	F:(B) ^a	22,37	22	12	40
MKW3S.....	141	cD	3,31	16	61	4

REFERENCES. – RS types: (a) Bahcall 1977; (b) Merrifield & Kent 1991; (c) Teague, Carter, & Gray 1990. Other references: (1) Abramopoulos & Ku 1983; (2) Bardelli et al. 1994; (3) Beers et al. 1991; (4) Beers & Tonry 1985; (5) Bothun & Schombert 1988; (6) Breen et al. 1994; (7) Burns et al. 1994; (8) Butcher & Olmer 1985; (9) Chapman, Geller, & Huchra 1988; (10) Coless & Hewett 1987; (11) Coless 1989; (12) David et al. 1993; (13) Davis et al. 1995; (14) Dickens, Currie, & Lucey 1986; (15) Dickens & Moss 1976; (16) Dressler 1980; (17) Dressler & Shectman 1988a; (18) Ebeling et al. 1996; (19) Edge & Stewart 1991a; (20) Elvis et al. 1992; (21) ENACS; (22) Ettori, Guzzo, & Tarenghi 1995; (23) Fabricant et al. 1993; (24) Gavazzi 1987; (25) Giovannelli, Haynes, & Chincarini 1982; (26) Gregory & Thompson 1978; (27) Gregory & Thompson 1984; (28) Gregory, Thompson, & Tifft 1981; (29) HEASARC Archive (NASA/Goddard) ; (30) Henriksen 1992; (31) Hill & Oegerle 1993; (32) Hintzen 1980; (33) Ikebe et al. 1994; (34) Jones & Forman 1984; (35) Kent & Sargent 1983; (36) Lauberts & Valentijn 1989; (37) Lucey & Carter, 1988; (38) Malumuth et al. 1992; (39) Metcalfe, Godwin, & Spenser 1987; (40) McHardy et al. 1981; (41) McMillan et al. 1989; (42) Moss & Dickens 1977; (43) Nilson 1973; (44) Oegerle & Hill 1992; (45) Ostriker et al. 1988; (46) Pierre et al. 1994; (47) Piro & Fusco-Femiano 1988; (48) Pinkney, Rhee, & Burns 1993; (49) Proust et al. 1992; (50) Quintana et al. 1985; (51) Rhee & Latour 1991; (52) Richter 1987; (53) Richter 1989; (54) Scodeggio et al. 1995; (55) Sharples, Ellis, & Gray 1988; (56) Sodrè et al. 1992; (57) Soltan & Henry 1983; (58) Teague, Carter, & Gray 1990; (59) Tifft 1978; (60) White & Fabian 1995; (61) Yamashita 1992; (62) Zabludoff et al. 1993; (63) Zabludoff & Zaritsky 1995; (64) Zwicky et al. 1961-1968.

In the same spirit, close clusters belonging to a given area are considered as a single field : the procedure we apply is supposed to retrieve individual clusters, but with objective centers and membership which may differ from traditional ones. Hence, we did consider in the same field six associations of clusters: A399-A401, A2063-MKW3S, A2197-A2199, A2634-A2666, A3391-A3395, and the whole region of the Shapley concentration (containing clusters A3558 and A3562).

Here we discuss only cluster fields which appear to have at least 50 galaxies with available redshift in the main peak of the velocity distribution (see next section). Relevant entries for the clusters considered are shown in Table 1. In Col. (1) we list the cluster names; in Col. (2) the number of galaxies with measured redshift in each cluster field; in Col. (3) the Rood-Sastry type given by Struble & Rood (1987) for Northern clusters and mainly by Struble & Ftaclas (1994) for Southern clusters; in Cols. (4) and (5) the redshift and magnitude references, respectively; in Cols. (6) and (7) the references for the adopted X-ray temperatures, hereafter T , and X-ray centers, respectively.

The X-ray temperatures indicated by an asterisk in Table 1 are rough estimates coming from the X-ray luminosity, hereafter L , by means of the $kT-L$ relation for the respective luminosity band. In particular, we used the relation by Edge & Stewart (1991a) for A1146. For A2197 and A2666 we used the relation $kT = 10^{-7} \cdot L(0.5 - 3KeV)^{0.17}$, which we obtained for the 28 clusters in common between the samples of David et al. (1993) and Henriksen (1992) by means of a direct linear regression.

3 THE METHOD

The purpose of this work is to point out any physical structure which is present within the analyzed sample. That implies, firstly, identifying the cluster itself within its own environment, and then detecting the presence of any subsystem lying in the region.

Due to the complex gravitational phenomena occurring in the region of a cluster, every physical structure is indeed characterized by correlations in space and velocity. Therefore, no individual structure identification can be performed without taking into account both kinds of information simultaneously. A direct three-dimensional analysis is not suitable, since redshifts inside a cluster are not pure distance parameters, owing to individual galaxy motions within the cluster. But redshifts still contain the traces of the dynamical processes that form or dissolve the systems. Depending on their nature, some processes will create local departures in the observables, the most usual ones being the mean and the standard deviation of the measured radial velocities (hereafter referred to respectively as the mean velocity and the dispersion σ). Hence, the analysis of local kinematics appears a very suitable tool to study physical processes occurring in galaxy clusters.

3.1 Investigation of local kinematics.

In this paper we call *structure* any galaxy association which may be physically connected through gravitational processes. As stated in a previous work (E94), an exploitable sign of the presence of these structures within their environment is a local departure in their mean velocities and dispersions. To emphasize the dynamical processes, which are present within a cluster of galaxies, we apply to each galaxy the weight term ρ which is a measure of that galaxy's kinematics. Such weights do work as local kinematical estimators since the structure quantities are computed within a limited area of radius R_s around each galaxy. The size of that area is related to the scale of the exploration (see below) and so, as previously stated, the crucial aspect of this analysis is the use of a multi-scale approach.

In the following, σ is the velocity dispersion and \bar{v} is the mean velocity of the n galaxies found in the area considered; the label *loc* refers to the local area of radius R_s , while the label *main* refers to the whole field.

The first estimator looks for the local departure of the velocity dispersion :

$$\rho_S = n \times (\sigma_{main}/\sigma_{loc})^2. \quad (1)$$

In this way, low values of local dispersions will produce high values of ρ_S .

The second estimator searches for local departures of the mean velocity :

$$\rho_V = n \times \left(\frac{\bar{v}_{loc} - \bar{v}_{main}}{\sigma_{main}} \right)^2. \quad (2)$$

Hence, prominent departures in the local mean velocity (e.g. by over a σ_{main}) will produce high values of ρ_V .

We normalize the weight terms ρ to their own mean values within the whole cluster:

$$\delta = \rho/\bar{\rho}. \quad (3)$$

In this way the value of δ does not depend on the cluster analyzed and its mean value is equal to one. Hence, values departing from unity directly identify the expected local effects.

Now we form a third estimator by computing the quadratic sum of the previous two :

$$\delta_P = \sqrt{\delta_S^2 + \delta_V^2}. \quad (4)$$

Finally we include a fourth estimator which is a local version of the Dressler parameter (Dressler & Shectman 1988b, hereafter D88) :

$$\delta_D = \frac{n_{loc}}{\sigma_{main}} \times \sqrt{(\bar{v}_{loc} - \bar{v}_{main})^2 + (\sigma_{loc} - \sigma_{main})^2}. \quad (5)$$

The estimator δ_P differs from δ_D since the normalization on ρ_S and ρ_V is done in eq. 4 before summing rather than after summing (as in eq. 5 for δ_D). In this way, the

estimator δ_P takes into account the departures in velocity and dispersion separately, while these two effects are confused in δ_D . It must be noticed that E94 did use the true Dressler parameter for nearly the same purpose. The main difference compared to the above δ_D is the restriction to a limited area around the galaxy considered, while the Dressler parameter systematically includes 11 neighbours in the computation, irrespective of the distance. The present work includes some clusters already considered in E94, in a few cases with the same dataset; using the kinematical weights mentioned above, we now expect to detect some new structures, e.g. those exhibiting discrepancies in the local dispersion or in the local mean velocity, whilst some previously detected structures will no longer appear significant, according to the more local definition of the present analysis.

The confidence level of the weight values is derived from the statistics computed on the set of values obtained throughout the whole cluster. High values correspond to prominent events, which occur around the galaxy considered. In this work we adopt the classical 3 s.d. threshold above the mean, which here refers to the statistics on the weight values. In order to obtain a more reliable estimate of the confidence level, we compute the distribution of weights for the whole sets of replicas (see below). In this way, for a given scale of analysis, we obtain a list of galaxies which are presumed to identify a structure.

3.2 Investigation of the subclustering processes.

Once the technique of individual weighting is applied, the spatial clustering of the galaxies needs to be quantified and estimated in terms of statistical validity. Therefore, we choose to perform the wavelet transform, which is particularly well suited for such purposes. The ability of galaxies to form structures is measured objectively with the wavelet coefficients in a multi-scale way.

The starting dataset for wavelet analysis is a bidimensional distribution of *weighted galaxies*, viz. a distribution of Dirac functions normalized to the weights δ_i . The analysis consists then in performing the transform by a wavelet function.

The details of analyzing a spatial distribution of galaxies with the wavelet transform have been extensively described in a series of previous papers (Escalera & MacGillivray 1995 and references therein). In this work we use the so-called Mexican Hat wavelet, which makes the transform at a given scale insensitive to the presence of a gradient at a much different scale (see also E94).

Therefore, the full-scale analysis is not sensitive to the presence of small-scale structures and leads to a definition of the main system.

The main procedure of our analysis consists in investigating simultaneously the local kinematics (weights) and the spatial clustering (wavelets). The two techniques are fully consistent with each other, since they are both objective (no free parameters and no preliminary assumptions are needed) and they both consist in a multi-scale analysis. The point is to use the same range of explored areas for the

weight terms and for the wavelet transform. When investigating a spatial distribution at a given scale s , the Mexican Hat explores areas roughly extended for $4s$. Thus, consistency with the weighting procedure is obtained by simply exploring an area of the same radius $R_s = 4s$ at the time of computing the weight values.

In practice we adopt a series of three successive scales : $s = 0.03125$, 0.0625 , and 0.09375 , leading to explored areas of radius R_s equal to 0.125 , 0.25 , and 0.375 , respectively, in units of the maximum radius of the field analyzed. Such a limited series appears sufficient to retrieve any substructure present in the sample. The only requirement for detecting conveniently a structure of a given size is to use an immediate upper and lower scale. It is not the aim of this work to detect the small pairs or triplets; thus the lower limit of 0.03125 does fulfill the purpose.

The membership of a given structure is the set of galaxies, within the explored area, selected by the weighting technique, i.e. galaxies which have significant weights ($|\delta - \bar{\delta}| \geq 3\sigma_\delta$, see § 3.1) and confirmed by wavelet analysis. Then, the estimate of structure size is determined on the identified members by computing the projected radius. Thus, it is possible that we may retrieve some structures which are smaller than the smallest wavelet scale we use. Throughout the present work, the wavelet scales we use lead to resulting structures with dimensions of about $1.5 h^{-1} Mpc$ (median value) for the main cluster, down to about $0.2 h^{-1} Mpc$ for the smallest substructures detected.

We preferred to use a relative array of scale sizes rather than a fixed one because we study clusters of different intrinsic sizes for which a fixed scale could have a different physical interpretation. For instance, $0.5 h^{-1} Mpc$ can be the measure for the global size of a poor cluster or the measure for a clump in a bimodal cluster. In our procedure the first step generally gives the cluster immediately, independently of its dimensions. Wavelet analysis does not require the use of a scale rigorously equal to the size of the structure, but it is only necessary to approach this value by close wavelet scales. Hence, the use of a fixed array of scale sizes rather than a relative one should not have strong repercussions on the determination of structure sizes if a similar range of sizes is examined. In particular, our evaluations of structure sizes depend on the values of kinematical weights and so they are not strictly linked to the choice of the array of wavelet scales.

The statistical significances are simply derived by comparing the wavelet coefficients obtained in the real field with those produced in a series of N replicas (see e.g. Escalera & Mazure 1992). The replicas are obtained by drawing independently the positions X_i and Y_i from the X and Y distributions of the sample studied and then by randomly reassigning the velocities. These replicas contain all the phenomena that can produce random associations of galaxies. By selecting the groups which do not appear in the replicas we simply separate the underlying physical processes from the random ones. Thus we finally arrive at the probability that the observed structure is not due to a randomly associating process or to projection effects.

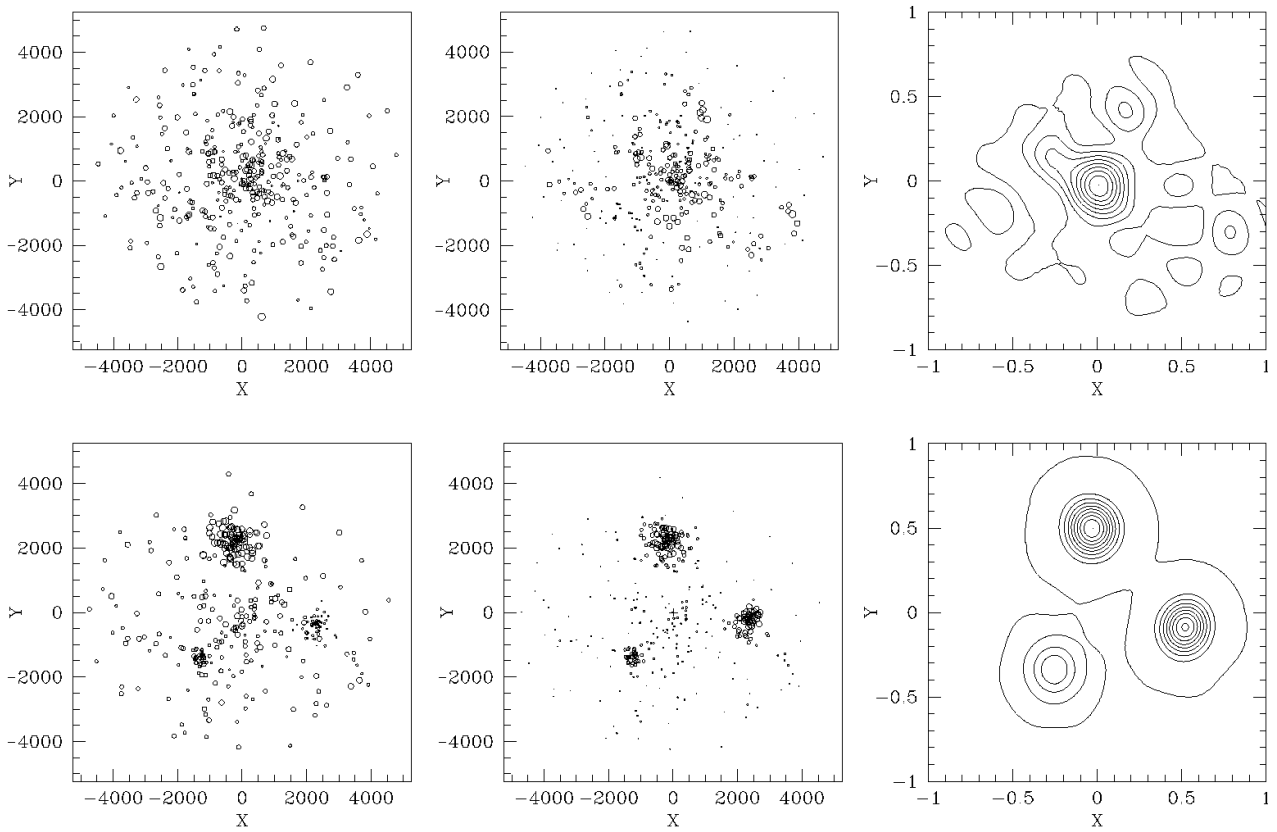


FIG. 1.— Illustration on a toy-model. A simulated regular cluster (Figures on the top) compared to a perturbed cluster (Figures on the bottom). Figures at the left show the distribution of galaxies: the symbol size increases towards low values of velocity. Substructures in perturbed cluster are thus clearly visible. Figures at center show the distributions of the weighted galaxies: the symbol size now increases towards high values of the weight δ_D . In the case of the perturbed cluster, the selection of the significant value locates departures in the local kinematics. On the contrary, in the regular cluster, none of the observed δ values is significant. Figures at the right show the wavelet images of the above weighted bidimensional maps, i.e. the isophotes of the wavelet coefficients. As above, the perturbed cluster shows significant features (compared to random simulations) which do correspond to the input substructures, while the regular cluster does not contain any significant features.

We point out that an appreciable improvement in the analysis comes from the fact that departures in mean velocity and in dispersion are investigated separately, by means of specific weight terms.

For each cluster we consider 4 weight terms at 3 different scales, obtaining in that way a series of 12 maps. We retain a structure if it appears significant in at least one of these maps.

The main results are the structure positions derived by the location of the local maximum of the wavelet coefficients, the full membership given by the list of galaxies responsible for the observed local departure in kinematics, and the significance level, which is the probability for the observed structure to be reproduced within the random replicas of the analyzed data. The membership identification makes possible a dynamical analysis of the structure.

3.3 Illustration on a toy model.

We include here an example of a practical application of the whole detection analysis to a toy model, with the only purpose of emphasizing the possibilities and the limits of our detection procedure. For a full illustration of our procedure, where we consider many alternative toy models by varying the positions, extents, and dynamics of the input substructures, we refer to Escalera & MacGillivray (1995) and references therein.

The simulations we use here consist in a regular cluster compared to a perturbed cluster. The regular cluster has a smooth symmetric density profile (viz. the so-called King profile) and a Gaussian velocity distribution. The second cluster, similar to the regular one in extension, population, and global kinematics, consists in a main fully regular structure (M) perturbed by a loose triplet (D) and

by three regular substructures (A,B,C) which are distinct from each other in population and extension and are inserted within the limits of M. The subgroups depart from M in terms of mean velocity and/or dispersion (see Table 2 and Figure 1).

TABLE 2

DETECTION IN A TOY MODEL

Structure	N_{gal}	X	Y	\bar{v}	σ	P_{SL}
INPUT						
total	353	0.0	0.0	14944	1759	
M	200	– 16.2	– 31.7	15070	1059	
A	75	– 12.2	493.0	12572	419	
B	50	508.3	– 9.0	17627	728	
C	25	–214.3	–208.5	15956	76	
D	3	203.0	403.0	12003	...	
OUTPUT						
M	196	– 13.5	– 27.1	15040	1066	...
A	75	– 12.0	490.8	12578	434	0.00
B	51	506.8	– 7.9	17602	754	0.00
C	28	–214.2	–209.6	15952	92	0.00
D	3	203.0	403.0	12003	...	0.01

As one can see in Table 2, A is almost completely detected, with one true object missing and one false object (interloper) included, and its dynamics is accurately obtained. B is fully detected with the addition of a single false object which does not significantly perturb the main dynamics of the structure. C is also fully detected, with the addition of 3 false objects, so its dispersion is slightly overestimated, though within the error bars, and its mean velocity remains acceptable since - by definition - the contaminating objects are related to the real dynamics of the subgroup. Finally, the close triplet D is detected with no contamination. The resulting main cluster M is obtained by subtraction of the detected substructures, and consequently appears very close to the input data: only 5 objects are missing (wrongly attributed to the substructures) and one is added. Then, as expected, no clump is significantly detected in the regular cluster.

In Table 2 we list the structure positions, i.e. center coordinates in arbitrary units with a maximum error of 7.8 units; the membership, which leads to the computation of the mean velocity \bar{v} and dispersion σ ; the significance level, i.e. the percentage of similar structures found in the simulations. Through the whole paper we used a series of 1000 simulations to compute the significance levels.

When showing the detection power of a method, it is also important to keep in mind its limits. We stress that the structures are detected if they depart significantly from the environment (cluster from field, or substructure from cluster), i.e. if \bar{v}_{loc} departs from \bar{v}_{main} by more than $0.3 \times \sigma_{main}$, and/or σ_{loc} is smaller than $0.8 \times \sigma_{main}$. Moreover, the membership is retrieved with an error of about 10%, i.e. one object out of 10 can be missed and/or replaced by a contaminating object.

Obviously, the position of the structure within the cluster and its relative extension affect the efficiency of the detection. In practice, structures that do not obey at least one of the above two criteria will be missed; e.g. structures

with low departures of \bar{v} are not significant if they are not well separated in the map. They just resemble projected random fluctuations of the 3-D distribution. On the contrary, structures that fulfill the two above conditions can be easily detected whatever their relative population and location within the cluster field may be.

3.4 Procedure on real data

The application to real data of the procedure described above requires a preliminary identification of the true cluster in the field. The full system identification therefore consists in a series of three successive stages arranged as follows.

1. Main Peak. Several methods have been proposed in the literature for identifying coherent physical systems in redshift surveys (see, e.g., Mazure et al. 1996). In this preliminary stage, however, we do not want to prematurely break up physical systems. We only want to identify obvious subsystems (fore- and background groups), keeping the dominant system intact for further three-dimensional analysis. In order to avoid unnecessary sophistication, we used the Poissonian Gap method, which is a simple and stable method for defining systems. The gap is the separation between adjacent galaxies in the velocity distribution. For each cluster field, gaps greater than the median value generally correspond to unrelated systems, as recently demonstrated by Katgert & al. (1996). Such conclusions do not depend on noise effects as long as the samples are complete enough and do contain a reasonable population (namely ≥ 30 galaxies). Both conditions are fulfilled in our dataset.

When more than one system is found in the field, for further analysis we retain only those with at least 50 galaxies.

2. Main System. The present stage introduces the three-dimensional analysis and consists in exploring the samples at a large scale ($s = 0.125$). In this way, the considered area approaches the whole field ($R_s = 0.5$); thus the local kinematics is close to that of the whole field. Therefore, at this stage, we spatially identify the true cluster within the selected main peak. Since in any case we combine positions and redshift information, the remaining background/foreground galaxies are also identified and removed. These galaxies initially belong to the main peak of the velocity distribution, but are indeed outside the spatial limits of the detected structure. In the case of bimodal clusters and of two distinct populations, which overlap in velocity, we can clearly separate them by combining galaxy positions with kinematic estimators. At this stage unconnected subsystems are listed and removed for further analysis.

3. Multi-scale analysis. We calculate the weights (described in § 3.1) for each galaxy by taking into consideration a surrounding area, whose size corresponds to the chosen scale. As previously stated, the multi-scale analysis consists in taking a series of decreasing scales.

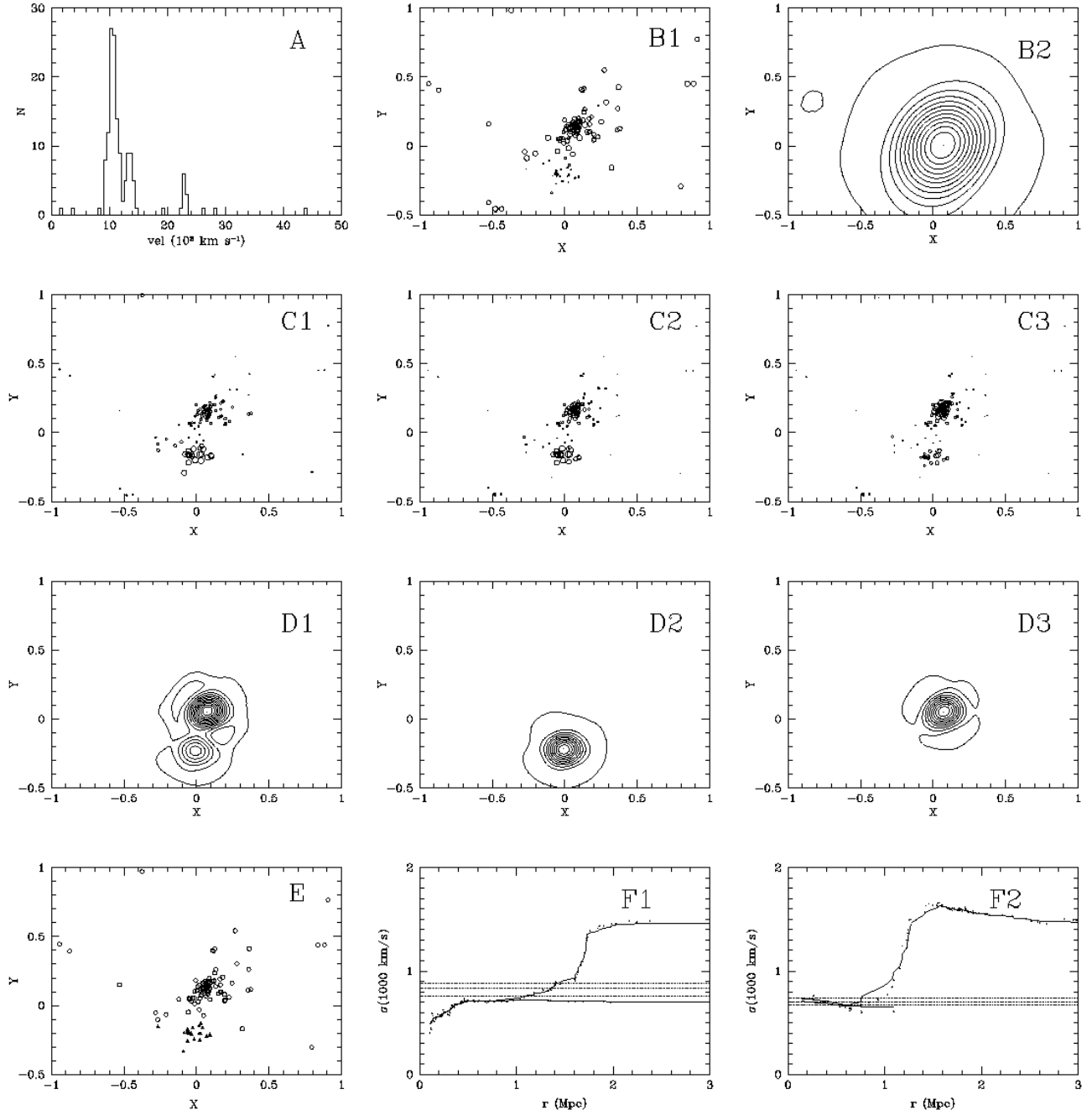


FIG. 2.— A real example: A2063-MKW3S field. (A) Selection by gapper procedure of the main peak in the redshift distribution (roughly from 9000 to 15000 km s^{-1}); (B) Spatial distribution of galaxies in the main peak (symbol sizes increases towards low redshifts) and corresponding isopleths of the wavelet coefficients, as a result of the large scale bi-dimensional analysis; (C) Substructure identification by applying the weight terms δ_D , δ_V , and δ_S respectively, with large symbols corresponding to large departure in the local kinematics; (D) Isopleths of the wavelet coefficients obtained through analysis of the *weighted* cluster as in C1, C2, and C3 respectively. Both structures are present in the δ_D image (D1), while the δ_V image (D2) shows only the background structure, whose departure in the local mean velocity is high. The δ_S image (D3) shows the main concentration; there are, in fact, no strong deviations from the local dispersion in this sample, so only spatial clustering is retrieved; (E) The membership of the two structures indicated by two different symbols; (F) Comparison between the velocity dispersion profiles of the initial main sample and the two selected structures, main concentration (F1) and background structure (F2), respectively. In computing the profiles the respective X-ray centers are used. The corresponding X-ray temperatures with their error bands are plotted for comparison.

The above procedure can be summarized with the following symbols:

- *field*, the initial sample (whole cluster field).
- *MP*, the main peak, which results from the Poissonian gap method.
- *US*, or *US1*, *US2*, etc., unrelated structures, are coherent systems unrelated to the cluster and are identified from the bi-dimensional analysis at the largest scale. An US structure is considered as a secondary main system if its population is at least $\sim 25\%$ of the primary main system (see below MS1, MS2).
- *MS*, the main system, which generally corresponds to the *identified cluster*.
- *MS1*, *MS2*, two comparable main structures, e.g. two clusters in the same field or individual lobes in the case of a bimodal cluster.
- *S* or *S1*, *S2*, etc., the successive substructures, outputs of the multi-scale structural analysis.
- *C*, the core structures, i.e. structures detected in the central cluster region, whose mean velocities do not significantly differ from the respective cluster mean velocities (i.e. the difference is less than the velocity dispersion of the cluster itself).

Sometimes we needed to analyze the effect of removing a substructure from the parent structure. We refer to the remaining galaxies by inserting a sign of subtraction between the symbols of structures, e.g. MS-S1-S2 if substructures S1 and S2 are removed from the MS structure.

For each cluster we have to examine twelve figures (four weights at three different scales). We illustrate the procedure described above by giving the complete set of figures for the field of A2063-MKW3S (see Figure 2). It consists of a main regular cluster with a poor background cluster which is only $\sim 3000 \text{ km s}^{-1}$ away and thus gives a clear representation of the way the method works.

4 THE DETECTED STRUCTURES

The results of our structural analysis (§ 3) of galaxy clusters are presented in Table 3, which also contains the basic kinematical properties of the detected structures. The structures mentioned have a confidence level $\geq 99.5\%$, i.e. less than 5 chances in 1000 of being due to a random configuration. In some few cases, however, we do include results for less significant structures which appear to be of some particular interest (as specified in Table 3). In principle, each structure corresponds to a physical structure. Artifacts and field contamination are not touched in the discussion.

We applied homogeneous procedures to the study of the detected structures. In order to determine the center of

structures, we used the two-dimensional application of the adaptive kernel method (e.g. Pisani 1993; Girardi et al. 1996 and reference therein).

Then, the projected radius R of the structures is determined as the maximum projected distance from the center for all the galaxies belonging to the structure.

We used robust mean and dispersion estimates computed by using the ROSTAT routines by Beers, Flynn & Gebhardt (1990). As an estimator of the Gaussianity of velocity distributions, we adopted the probability P_W associated with the W-test (Shapiro & Wilk 1965). Remarkably, non-Gaussian velocity distributions could be due to the presence of substructures, but also to the presence of velocity anisotropies (Merritt 1987); thus the absence of Gaussianity is only a *sign* of possible substructures.

Hence, for all the detected structures, Table 3 gives the following entries: the field name and their nature, indicated by symbols as described in § 3.4; the number of involved galaxies N ; α and δ coordinates of the galaxy density center, epoch 1950; the overall projected radius R (in $h^{-1} \text{ Mpc}$); the mean velocity \bar{v} ; the P_W probability and velocity dispersion σ (in km s^{-1}) with the respective bootstrap errors; the name of the *identified cluster*: this identification is particularly useful when the field contains more than one cluster.

The spatial distributions of galaxies of *identified clusters*, which show internal structures (substructures and/or core structures), are displayed in Figure 3.

For each *identified cluster*, and other interesting structures, in Figure 4 we show the respective velocity dispersion profile, hereafter VDP, which, at a given radius, is the averaged l.o.s. velocity dispersion within this radius. The horizontal lines in Figure 4 show the values of the velocity dispersion obtained from the temperatures (see Table 1) under the condition of a perfect galaxy/gas energy equipartition, i.e. with $\beta = \sigma^2 / (kT / \mu m_p) = 1$, where μ is the mean molecular weight and m_p the proton mass (see e.g. Sarazin 1986 and references therein). If both galaxies and gas are in dynamical equilibrium within the cluster, one expects that the observed σ will coincide with that obtained from T .

The square of l.o.s. velocity dispersion, as computed on the whole cluster, is a third of the squared spatial velocity dispersion independently of the presence of velocity anisotropies in galaxy orbits (e.g. The & White 1986; Merritt 1988). However, velocity anisotropies can strongly influence the l.o.s. velocity dispersion, as computed on the central cluster region. In particular, the presence of circular orbits in the central cluster region, as expected in a relaxed cluster, produces a VDP decreasing towards the cluster center (e.g. Sharples et al. 1988). On the other hand, the presence of radial orbits in the external region, as expected for a cluster with galaxy infall, produces a VDP increasing towards the cluster center (e.g. Merritt 1987). The VDPs of our *identified clusters* are generally flat in the external regions.

TABLE 3
DETECTED STRUCTURES

Sample name		N	Center 1950 (α, δ)	R (Mpc)	$\langle V \rangle$ (Km/s)	P_W	σ (Km/s)	Identified cluster
A0085.....	MP=MS	124	003904.9–093356	1.74	16605	0.1	1015 (– 72, + 83)	A85
	S	7	003906.5–093528	0.22	13869	32.7	352 (– 17, +252)	
A0119.....	MP=MS	123	005345.9–013125	1.26	13258	7.5	769 (– 61, + 69)	
A0151.....	MP	95	010621.2–154039	1.73	15062	< 0.1	1860 (–133, +108)	
	MS1	65	010621.4–154036	1.59	15952	63.5	708 (– 55, + 69)	A151
	MS2	28	010625.5–161408	0.82	12317	47.8	391 (– 43, + 77)	
A0193.....	MP=MS	56	012228.2 082619	0.89	14559	26.0	726 (– 61, + 78)	A193
	S	4	012236.2 082328	0.04	14648	8.2	171 (– 33, +162)	
A0194.....	MP	156	012317.5–013644	4.55	5348	< 0.1	579 (– 76, +185)	
	US1	16	012053.1 012307	3.85	9683	22.7	490 (– 52, + 90)	
	US2	15	012033.1–005137	4.94	8381	7.6	619 (– 40, +128)	
	MS	121	012317.6–013640	4.55	5354	7.6	426 (– 31, + 46)	A194
	S1	3	013129.7–011852	
	S2	7	011022.8–003321	0.42	5390	91.1	178 (– 23, + 59)	
	C	19	012319.2–013553	0.98	5279	10.3	249 (– 29, + 43)	
A0262.....	MP	83	014951.1 355314	5.77	4904	12.9	538 (– 37, + 54)	
	MS	48	014949.1 355310	2.53	4881	23.8	528 (– 42, + 59)	A262
A0399–401....	MP	214	025613.6 132434	3.72	21838	10.0	1201 (– 45, + 70)	
	MS1	86	025612.8 132433	1.99	21901	15.0	1012 (– 60, + 76)	A401
	MS2	79	025507.3 124755	1.44	21151	1.4	961 (– 55, + 71)	A399
A0426.....	MP	126	031621.8 412155	2.65	5243	3.7	1239 (– 97, +115)	
	MS	122	031621.8 412155	2.64	5228	68.2	1138 (– 80, + 92)	A426
	C	37	031624.1 412200	0.53	5081	37.9	1154 (– 99, +133)	
A0539.....	MP	177	051917.4 032341	13.19	7061	< 0.1	2415 (– 99, + 59)	
	MS1	65	045617.1–003552	9.89	4478	< 0.1	382 (– 53, + 96)	
	C1	25	045616.5–003541	2.73	4428	59.4	267 (– 27, + 40)	
	MS2	85	051357.3 062413	13.72	8619	6.6	449 (– 39, + 57)	
	C	19	051733.3 063202	2.60	8797	7.1	227 (– 43, + 70)	A539
A0539*.....	C	36	051355.6 062334	0.36	8652	27.6	985 (– 76, +108)	
	C1	23	051354.0 062655	0.36	8112	11.1	620 (– 85, + 89)	
	C2	13	051409.0 062758	0.49	9709	11.8	402 (– 36, + 78)	
A0548.....	MP	341	054326.9–255739	2.61	12416	0.8	842 (– 24, + 29)	
	MS1	190	054326.8–255738	1.51	12603	0.2	880 (– 31, + 40)	A548SW
	S1	12	054112.6–255734	0.16	11645	68.0	691 (– 83, +136)	
	S2	43	054327.3–255726	0.56	13047	5.3	657 (– 63, + 63)	
	S3	17	054233.7–263538	0.41	11862	63.4	303 (– 33, + 61)	
	S4	17	054226.8–260540	0.48	12192	22.2	643 (– 49, + 96)	
	MS2	149	054636.5–253110	1.16	12167	< 0.1	680 (– 26, + 30)	A548NE
A0754.....	MP	89	090711.0–093108	2.64	16257	< 0.1	817 (– 77, +130)	
	US	8	090535.2–094736	0.72	15889	10.0	477 (– 89, +385)	
	MS	38	090708.3–093049	1.42	16428	0.7	495 (– 56, + 82)	
	MS1	22	090618.7–092155	0.76	16218	0.4	409 (– 17, +109)	A754NW
	MS2	16	090710.1–093019	0.88	16717	3.9	531 (– 92, +110)	A754SE
	C	8	090709.9–093023	0.90	16950	12.9	607 (– 61, +118)	
A1060.....	MP=MS	94	103411.4–271436	2.27	3752	8.2	634 (– 41, + 45)	A1060
	S	5	103217.8–281905	0.05	3402	0.7	130 (– 2, + 22)	
	C	14	103414.0–271456	0.27	3881	13.6	748 (– 74, +117)	
A1060*.....	MP=MS	125	103411.6–271442	2.26	3739	17.8	633 (– 32, + 47)	
	C	40	103411.7–271428	0.79	3690	3.9	780 (– 51, + 63)	
A1146.....	MP=MS	61	105850.1–222806	1.72	42646	73.7	1028 (– 96, + 93)	A1146
A1185.....	MP	69	110802.2 285803	4.51	9127	1.8	1240 (– 90, +123)	
	MS	55	110802.3 285803	4.64	9470	3.2	786 (– 54, + 54)	A1185
	C	23	110744.8 285746	1.27	9344	22.4	567 (– 46, + 88)	
A1367.....	MP=MS	68	114137.4 200601	0.98	6432	40.0	838 (– 68, + 81)	A1367
	S	6	114119.8 201415	0.09	6391	49.3	330 (– 22, +103)	
A1631.....	MP=MS	71	125020.6–150453	1.96	13962	48.9	703 (– 47, + 54)	A1631
	C	15	125019.7–150434	0.65	13583	18.7	530 (– 76, +100)	
	C1	6	125019.5–150431	0.13	13704	41.0	310 (– 56, +131)	
A1644.....	MP	91	125444.4–170748	1.98	14120	14.1	927 (– 78, + 89)	
	MS	84	125446.2–170939	1.90	14020	76.7	763 (– 50, + 64)	A1644
A1736B.....	MP	63	132426.5–265337	2.14	13812	4.7	976 (– 64, + 66)	
	MS	51	132428.3–265435	1.54	13594	2.6	824 (– 47, + 65)	A1736B
A1795.....	MP	85	134632.4 264905	1.79	18888	0.1	873 (– 75, +121)	
	MS	83	134632.4 264905	1.79	18885	56.4	828 (– 72, + 88)	A1795
	C	28	134629.9 264825	0.41	18833	19.8	623 (– 67, + 89)	
A1809.....	MP	60	135025.2 052241	1.66	23696	37.1	758 (– 65, + 86)	
	MS	54	135025.1 052241	1.34	23737	4.7	501 (– 35, + 40)	A1809
A1983.....	MP	81	145038.2 165346	1.82	13471	< 0.1	634 (– 70, +132)	
	MS	75	145038.2 165346	1.70	13492	0.7	514 (– 43, + 52)	A1983
	S	5	145058.4 165154	0.23	12606	50.7	253 (– 42, +130)	
A2052.....	MP	51	151418.3 071335	1.12	10553	32.7	641 (– 56, + 95)	
	MS	46	151416.8 071246	1.09	10459	9.1	561 (– 73, + 87)	A2052
A2063–.....	MP	127	151911.5 075400	6.76	10934	< 0.1	1404 (–123, +148)	
–MKW3S	MS1	91	152037.8 084742	5.15	10535	4.4	679 (– 46, + 49)	A2063
	S	7	151922.8 083508	0.34	11670	57.2	997 (– 74, +383)	
	MS2	26	151911.4 075356	1.33	13499	48.1	603 (– 59, + 61)	MKW3S
A2107.....	MP=MS	68	153729.6 215805	1.00	12337	64.0	684 (– 60, + 79)	A2107
A2124.....	MP	62	154257.0 361433	1.21	19663	52.7	872 (– 67, + 96)	
	MS	60	154259.0 361502	1.21	19619	20.9	809 (– 60, + 73)	A2124
A2151.....	MP	100	160311.4 175344	1.61	11034	51.3	801 (– 46, + 64)	
	MS	98	160311.6 175344	1.61	11011	12.8	762 (– 49, + 47)	A2151
	S1	19	160318.1 175413	0.42	10288	30.2	644 (– 68, + 81)	
	S2	29	160337.3 181556	0.66	11259	79.0	490 (– 47, + 74)	
	S3	5	160419.9 175429	0.12	11786	45.7	219 (– 17, +115)	
A2197–2199....	MP	78	162835.9 404423	13.59	9171	86.7	686 (– 48, + 69)	
	MS	66	162835.9 404357	3.59	9094	20.8	635 (– 41, + 65)	
	(MS1)	37	162705.2 394240	3.24	9303	54.2	686 (– 62, + 88)	A2199
	(S1)	4	162918.5 395620	0.17	8883	94.0	413 (–100, +149)	
	(MS2)	30	162835.1 404502	2.47	8988	13.5	585 (– 84, + 72)	A2197
	(S2)	4	162654.2 411600	0.10	9924	7.3	695 (– 53, +724)	
A2634–2666....	MP	300	233606.5 264536	13.76	9074	< 0.1	1409 (– 82, +120)	
	MS	264	233606.5 264536	5.63	9120	0.9	1145 (– 63, + 82)	A2634=
	S1	26	234829.4 265735	1.26	8079	50.3	386 (– 63, +111)	=MS-S1-S2
	S2	22	233806.7 263409	2.35	11494	4.9	377 (– 25, + 58)	A2666
A2670.....	MP	115	235139.9–104117	1.11	22904	5.4	1010 (– 70, + 85)	
	MS	111	235139.9–104117	1.11	22933	14.9	918 (– 47, + 65)	A2670
A2670*.....	MP	79	235140.0–104148	0.29	22867	25.4	1103 (– 67, + 79)	
	US	8	235129.5–104210	0.10	21096	57.9	443 (– 61, +153)	
	MS	68	235140.7–104151	0.30	23026	4.0	912 (– 66, + 65)	
A2717.....	MP	53	240035.0–361229	1.26	14715	47.7	488 (– 38, + 49)	
	MS	52	240036.6–361219	1.26	14703	11.0	467 (– 35, + 38)	A2717
	C	18	240033.8–361257	0.47	14276	9.7	364 (– 33, + 47)	
A2721.....	MP	83	000334.6–345928	1.61	34356	< 0.1	1092 (–148, +249)	
	MS	75	000335.0–345940	1.59	34292	21.6	841 (– 63, + 90)	A2721

TABLE 3 — *Continued*

Sample Name	<i>N</i>	Center 1950 (α, δ)	<i>R</i> (Mpc)	$\langle V \rangle$ (Km/s)	P_W	σ (Km/s)	Identified Cluster	
A2877.....	MP	97	010734.9–461300	1.09	7267	2.7	973 (– 77, + 82)	A2877
	MS	86	010735.8–461308	1.04	7111	51.3	744 (– 51, + 63)	
	C	16	010730.4–461430	0.14	6779	62.5	447 (– 42, + 65)	
	S	7	010645.0–460347	0.11	7455	40.8	345 (– 27, +108)	
A3128.....	MP	186	032927.9–524045	2.39	17996	11.7	869 (– 47, + 67)	A3128
	US	22	032620.7–531801	1.54	18006	27.3	388 (– 74, + 95)	
	MS	157	032927.5–524035	2.14	17957	14.8	841 (– 44, + 51)	
	C	61	032929.6–524017	0.98	17675	1.9	685 (– 42, + 54)	
A3266.....	MP	130	043007.3–614030	1.33	17811	78.3	1154 (– 67, + 92)	A3266
	US	23	043215.8–612750	0.43	17512	59.4	528 (– 52, + 72)	
	MS	96	043026.8–613347	1.04	17832	8.3	1138 (– 74, + 94)	
A3376.....	MP=MS	77	060037.9–395622	2.29	13909	95.3	737 (– 57, + 88)	A3376
	S	11	060034.1–395642	0.92	14156	18.1	313 (– 39, +117)	
A3391–3395....	MP	211	062636.0–542435	2.64	15424	< 0.1	1241 (– 47, + 63)	A3395
	MS1	151	062632.2–542426	2.54	14890	2.4	823 (– 43, + 51)	
	C1	87	062627.9–542433	0.80	15107	16.0	740 (– 51, + 56)	
	MS2	53	062514.2–533951	2.64	17081	5.2	786 (– 53, + 78)	A3391
	C2	29	062515.5–533941	0.75	16476	18.1	581 (– 40, + 73)	
A3526.....	MP	112	124659.4–410644	1.49	3623	< 0.1	930 (– 46, + 46)	A3526
	MS1	67	124636.1–410224	1.14	3005	0.4	562 (– 34, + 54)	
	MS2	44	124936.3–410055	2.21	4572	40.2	294 (– 28, + 40)	A3526B
	C	15	124933.8–410105	0.46	4749	60.8	150 (– 19, + 37)	
A3526*.....	MP	102	124710.0–410844	1.68	3533	0.3	883 (– 45, + 47)	A3562
	MS1	69	124700.3–410442	1.48	3063	0.7	520 (– 39, + 49)	
	S	8	124704.0–405238	0.58	2078	73.1	183 (– 24, + 50)	
	MS2	31	124928.2–410138	1.82	4561	32.9	249 (– 25, + 24)	
	C	6	124930.0–410255	0.45	4856	57.8	96 (– 10, + 28)	
	MP	482	132501.2–311324	4.61	14277	< 0.1	1075 (– 36, + 48)	
Shapley..... concentration	US1	21	132056.8–312950	0.67	14340	82.1	583 (– 64, + 91)	A3562
	US2	83	133208.6–312241	1.67	14008	0.3	1416 (–134, +125)	
	(US2S)	20	133046.0–311739	0.57	14098	42.7	717 (– 70, + 87)	
	MS	373	132501.2–311324	2.59	14292	12.4	994 (– 33, + 45)	
	S1	44	132625.5–310215	0.71	15044	0.5	755 (– 73, + 78)	
	S2	46	132822.5–313110	0.78	13745	< 0.1	725 (– 50, + 85)	
A3667.....	S3	95	132459.6–311307	0.95	14320	1.6	735 (– 41, + 49)	A3558
	MP	163	200653.5–564955	2.66	16664	59.7	1094 (– 55, + 81)	
		MS	152	200653.5–564955	2.67	16683	68.8	1052 (– 66, + 72)
	S	11	201002.4–570835	0.39	15943	76.4	487 (– 60, +102)	
A3716.....	MP	92	204813.4–525820	2.20	13684	9.4	843 (– 54, + 54)	A3716S
	MS	62	204813.3–525822	1.06	13433	9.6	817 (– 47, + 65)	
A3888.....	MP	74	223130.2–375948	1.50	45444	1.0	1826 (–180, +248)	A3888
	MS	64	223132.2–375938	1.53	45682	9.5	1307 (– 92, +100)	
A4038.....	MP=MS	43	234505.4–282443	0.46	8630	1.0	898 (–116, +112)	A4038

NOTE. – The bracketed structures are detected at a c.l. < 99.5%. The samples marked by an asterisk are alternative initial samples, with a lower completeness level or a smaller extension.

This suggests that we are considering a region large enough so that the effects of (possible) velocity anisotropies are already averaged and hence the global value of galaxy velocity dispersion is independent of possible velocity anisotropies. Therefore, we take the VDP-value corresponding to the external region as our estimate of σ . In this paper we interpret the observed behaviours of the VDP in internal region as being due to the presence of velocity anisotropy although they could be explained also by peculiarities of internal relative distribution of mass and galaxies (e.g. Merritt 1987).

5 GENERAL RESULTS AND DISCUSSIONS

Our fairly large sample of clusters enables us to draw some general results in a statistical way. In the following analyses, we do not consider clusters A2197, A2199, and A3562, which are identified with a small statistical significance, and cluster A539, whose internal structure is not clearly understood.

These analyses concern the “identified clusters” which, in 21 cases, do not correspond to the main peak. For these 21 clusters, our cluster identification always leads to a reduction in the value of σ ; the σ of the main peak shows a mean overestimate of about 18%, with a maximum of 58% for cluster A1185.

In general, after the cluster identification, the velocity dispersion profile (VDP) becomes less noisy and flatter in the outer regions. The VDP drastically changes in the case

of fields which contain more than one system (see Figure 2).

5.1 Morphological classification

One of our main aims is the classification of the structure of galaxy clusters in order to better understand their morphology. In Table 4 we attempt a classification based on the substructures detected within each cluster area. We only classify the samples identified as *identified clusters*, without considering the initial cluster fields whose morphologies depend on the extension of the observed area.

We introduce some morphological categories, which depend on the cluster appearance at different scales.

We define three categories:

Unimodal: these clusters appear as single systems at large scales.

Bimodal: these clusters (A754, A548, A3526) show two main systems at large scales. Moreover, we consider also A1736 and A3716 to be bimodal clusters as they are well known to be bimodal in the literature, although in this paper we analyzed only one of their components.

Complex: these clusters show substructures which involve a large part of the main system itself (cluster A2151 and the clump denominated A548SW).

For clusters analyzed, we list in Table 4 the presence of substructures and/or any kind of irregularity detected in our analysis (i.e. a non-Gaussian velocity distribution, $P_W < 5\%$, and/or a cD galaxy with peculiar velocity).

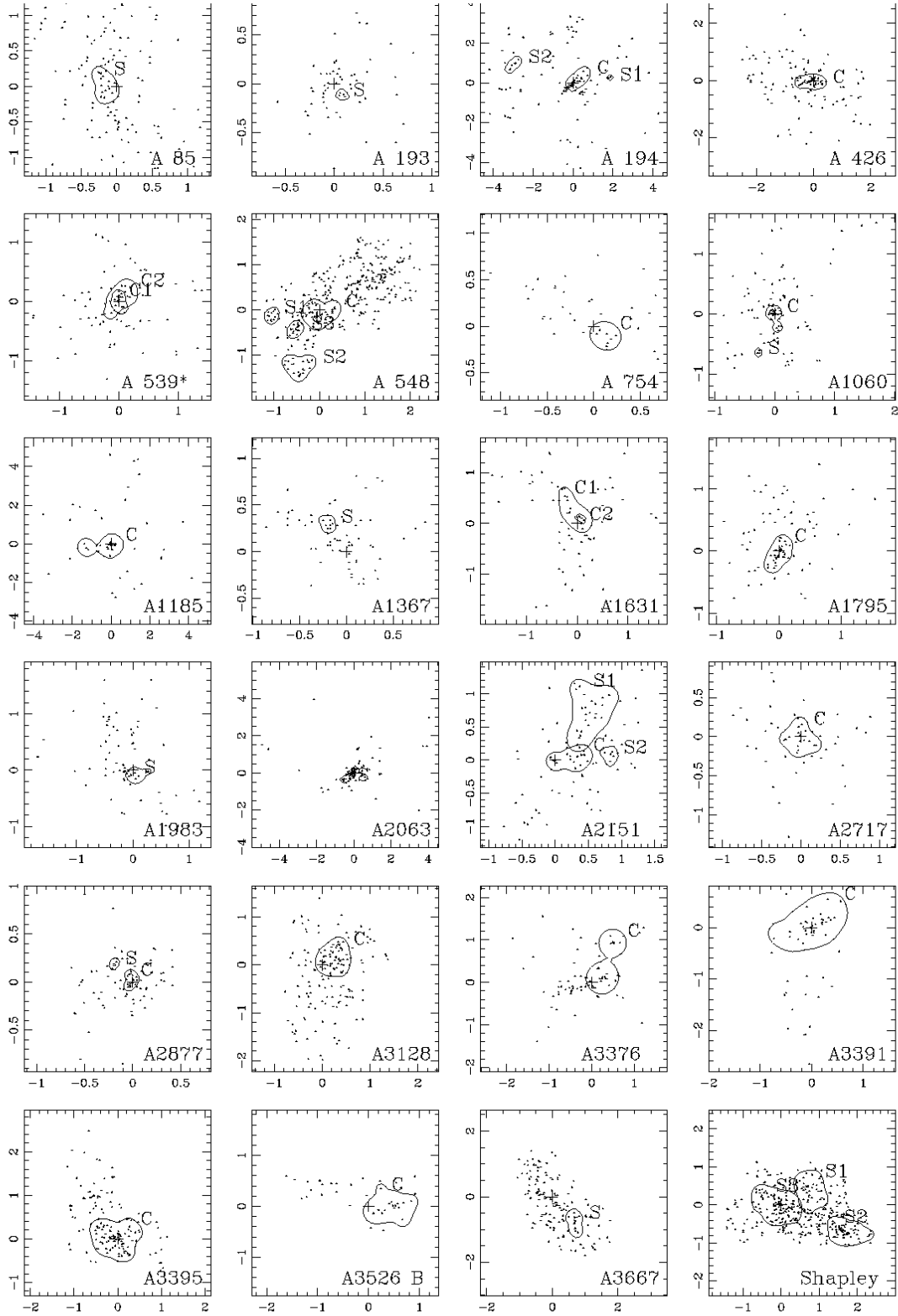


FIG. 3.— Spatial distribution of galaxies of *identified clusters*, which have internal structures, are shown. Contours contain all the members assigned to respective substructures. X-ray centers are indicated by crosses.

TABLE 4
MORPHOLOGICAL CLASSIFICATION

Cluster (1)	Morphology (2)	Irregularities (3)	Cluster (1)	Morphology (2)	Irregularities (3)
A0085	Uni	sub, $P_W < 5\%$	A2052	Uni	...
A0119	Uni	...	A2063	Uni	sub, pec. cD, $P_W < 5\%$
A0151	Uni	...	A2107	Uni	pec. cD
A0193	Uni	sub	A2124	Uni	...
A0194	Uni	sub	A2151	Comp	sub
A0262	Uni	...	A2634	Uni	$P_W < 5\%$
A0399	Uni	$P_W < 5\%$	A2666	Uni	...
A0401	Uni	pec. cD	A2670	Uni	pec. cD
A0426	Uni	...	A2717	Uni	...
A0548	Bi	...	A2721	Uni	...
SW	Comp	sub, $P_W < 5\%$	A2877	Uni	sub
NE	Uni	$P_W < 5\%$	A3128	Uni	...
A0754	Bi	...	A3266	Uni	...
NW	Uni	$P_W < 5\%$	A3376	Uni	...
SE	Uni	$P_W < 5\%$	A3391	Uni	pec. cD
A1060	Uni	sub	A3395	Uni	...
A1146	Uni	pec. cD	A3526	Bi	...
A1185	Uni	$P_W < 5\%$	A	Uni	$P_W < 5\%$
A1367	Uni	sub	B	Uni	...
A1631	Uni	...	A3558	Uni	pec. cD, $P_W < 5\%$
A1644	Uni	pec. cD	A3667	Uni	sub
A1736	Bi	...	A3716	Bi	...
A	N
B	Uni	$P_W < 5\%$	S	Uni	...
A1795	Uni	...	A3888	Uni	...
A1809	Uni	$P_W < 5\%$	A4038	Uni	$P_W < 5\%$
A1983	Uni	sub	MKW3S	Uni	...

NOTE. — “Uni”, “Bi”, “Comp”, mean unimodal, bimodal, and complex, respectively. “Sub” indicates the presence of substructures, “pec. cD” the presence of a cD galaxy with peculiar velocity, and “ $P_W < 5\%$ ” a low probability of Gaussianity of the velocity distribution.

Here a cD galaxy is defined as having a *peculiar* velocity by adopting the robust test by Gebhardt & Beers (1991), and considering the 95% c.l.

For a limited number of clusters we made a comparison with the results obtained by Gurzadyan & Mazure (1996) by means of a recently developed method, which enables one to study the hierarchical properties of the subsystems by taking into account the positions, redshifts and magnitudes of cluster galaxies, and thus to assign the full system membership (see Gurzadyan, Harutyunyan, & Kocharyan 1994). For six clusters in common with our sample, there appears to be fair agreement in the identification of the main system and of the most prominent substructures.

Out of 44 clusters, we classify five clusters as bimodal, one as complex, and the others as unimodal. In 9 of the 38 unimodal clusters we clearly detect the presence of small-scale substructures and there is some sign of them in 12 others. Hence, we detect substructures in about one third (15/44) of our clusters. This is in broad agreement with previous statistical works which employ different techniques (Geller & Beers 1982; Dressler & Schectman 1988b; Jones & Forman 1992).

Our cluster sample is, however, slightly biased towards more regular clusters. In fact about half of our clusters are cD ones, which are usually better studied, while we verified that in Northern Abell Catalog only $\sim 20\%$ of the nearby (Abell distance class ≤ 4) clusters are classified as cD. Hence, the result of our classification may not strictly be representative of the Universe.

5.2 Optical and X-ray results

In the detailed discussion of individual clusters (see the appendix) and in Figure 4 we have often compared our results obtained from optical data with those coming from X-ray studies. Here we may summarize some main points. We consider 42 clusters or clumps for which there is a corresponding unambiguous identification in X-ray maps. Therefore we do not consider clusters A754, A2151, A3526. We found that the mean distance between X-ray and optical centers is $0.11 h^{-1} \text{ Mpc}$, which is roughly the typical uncertainty in the estimate of cluster centers (e.g. Beers & Tonry 1986; Rhee & Latour 1991).

In our sample the mean (absolute) percent difference between the σ -value and the corresponding T -value is about 17%. This discrepancy is consistent with typical errors on σ (8%), and on T (12%), for 29 clusters having a direct measure of T . The other clusters, whose T is estimated by X-ray luminosity, are supposed to be affected by larger errors on T . Figure 4 shows that σ and T agree well for most clusters, with two exceptions (A119 and A1060), whose measures differ by more than two s.d.. For A2634 the agreement is acceptable within the presumably virialized region. The general good agreement between global X-ray and optical cluster properties make us confident in assuming dynamical equilibrium of both galaxy and gas components within the cluster potential and thus in using the virial mass estimator. The mean value of β is 0.90 with a rms = 0.29.

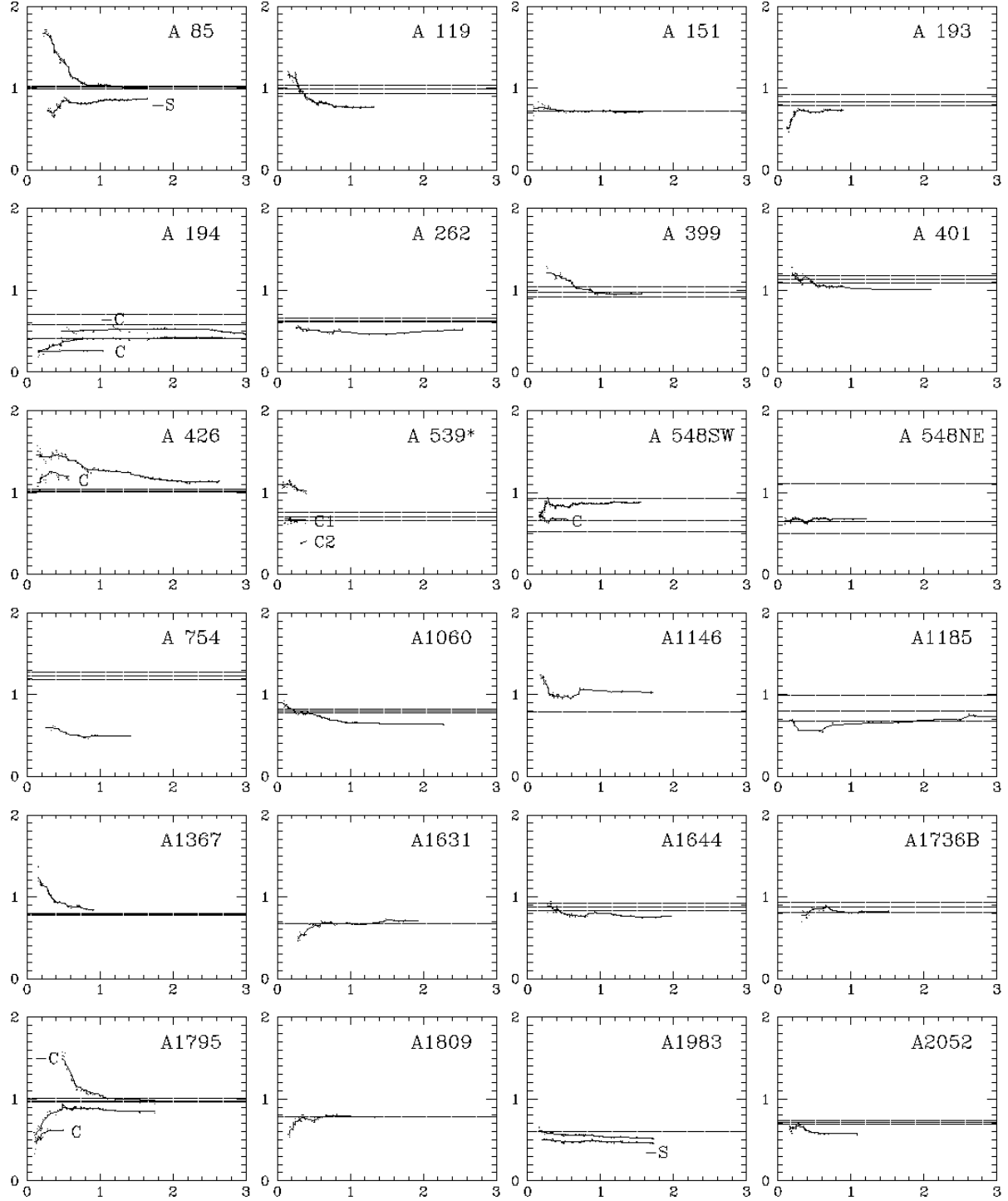


FIG. 4.— The velocity dispersion profiles (VDP), where the dispersion at a given radius is the average l.o.s. velocity dispersion within this radius. The VDP units are 10^3 km s^{-1} , and distance from the center is expressed in Mpc. The center is generally the X-ray center if not specified otherwise in the text. The first point represents the σ as computed for the ten galaxies, which are closest to the cluster center. Subsequently points are computed considering one more galaxy each time. A smoothed line is also superimposed. The horizontal lines show the values of σ , and the respective error bands obtained from the X-ray temperatures (see Table 1) on the condition of perfect galaxy/gas energy equipartition, i.e. $\beta = 1$.

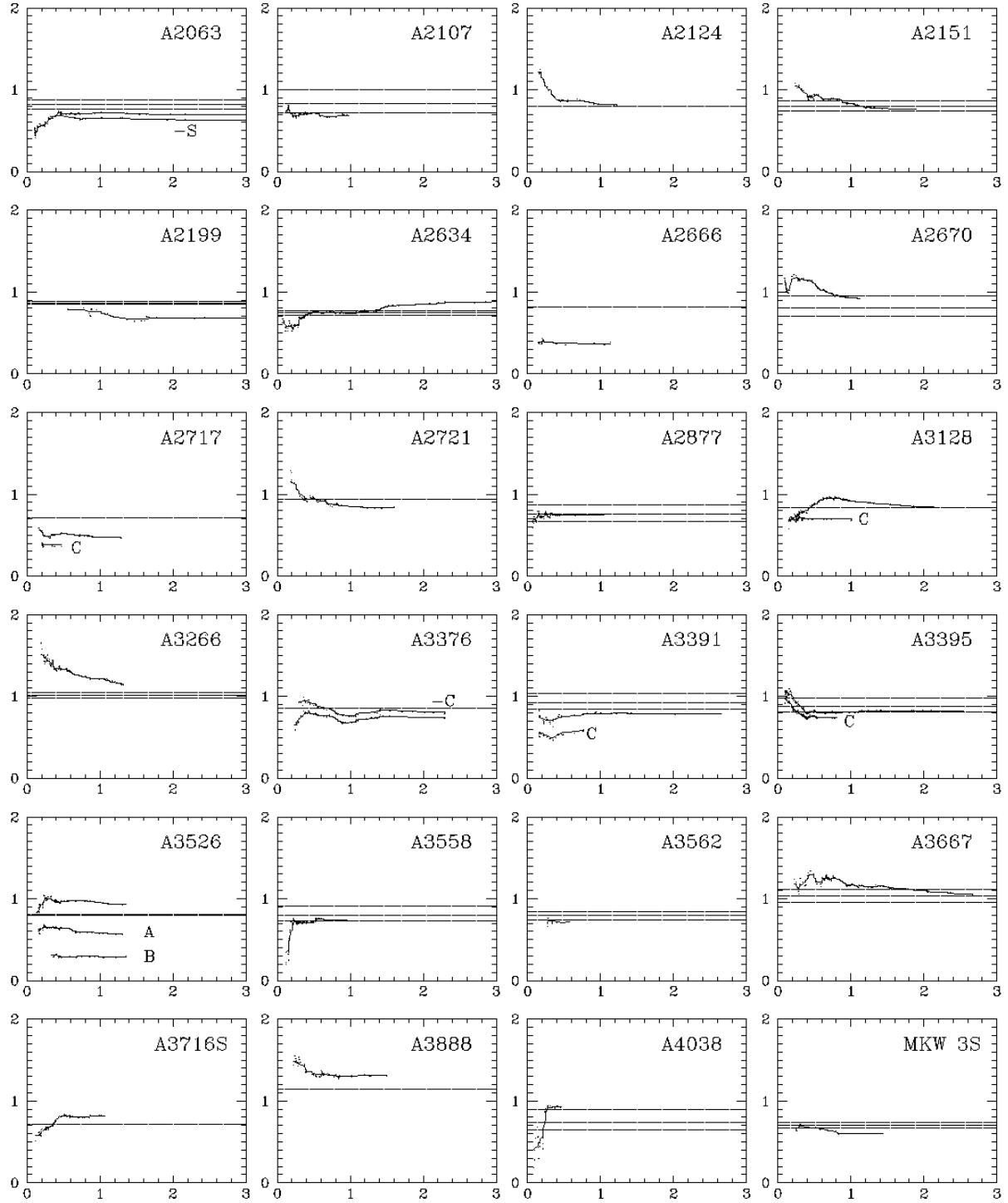


FIG. 4.— Continued.

5.3 Unimodal Clusters

In the case of 9 unimodal clusters, which show the presence of substructures, we analyzed the effect of substructures on the kinematics and dynamics of clusters by comparing the values of σ and mass computed before and after rejection of the detected substructures. We adopted the

standard virial mass (see e.g. Giuricin, Mardirossian, & Mezzetti 1982), which is strictly valid only if the mass distribution follows galaxy distribution (e.g. Merritt 1987; Merritt 1988). However, the same hypothesis is also assumed in other usual mass estimators, e.g. in the projected mass estimator (Heisler, Tremaine & Bahcall 1985) used by B95, whose results will be compared with ours.

TABLE 5
THE EFFECT OF SUBSTRUCTURES

Cluster (1)	σ (Km/s)		Mass $_{<1.5Mpc}$ ($10^{14}M_{\odot}$)		R_v (Mpc) (6)	Mass $_{<R_v}$ ($10^{14}M_{\odot}$)	
	before (2)	after (3)	before (4)	after (5)		before (7)	after (8)
A0085	995(−77, +88)	853(−47, +59)	13.4±2.1	6.5±1.1	1.66	13.4±2.1	10.8±1.5
A0193	723(−58, +90)	751(−64, +78)	3.6±0.9	4.1±0.9	1.12	3.6±0.9	4.1±0.9
A0194	389(−45, +54)	389(−45, +54)	1.4±0.4	1.4±0.4	0.54	0.8±0.3	0.8±0.3
A1060	639(−39, +49)	649(−42, +49)	3.8±0.5	3.8±0.6	1.04	3.5±0.5	3.5±0.5
A1367	836(−69, +79)	881(−59, +80)	5.2±1.1	6.2±1.0	0.99	5.2±1.1	6.2±1.0
A1983	528(−25, +60)	472(−31, +56)	3.1±0.6	2.6±0.6	0.59	1.8±0.4	1.2±0.3
A2063	701(−51, +68)	639(−47, +72)	4.0±0.8	3.1±0.7	1.10	3.7±0.8	2.9±0.7
A2877	741(−55, +59)	766(−59, +62)	3.2±0.6	3.5±0.7	0.94	3.1±0.6	3.3±0.7
A3667	1141(−76, +39)	1092(−70, +86)	17.1±2.4	17.0±2.5	1.74	17.5±2.4	18.4±2.6

The virial mass estimate does not require any assumptions about the isotropy of galaxy orbits, since each possible effect vanishes by averaging the velocity dispersion over the whole cluster sample (Merritt 1987). The virial mass is fully meaningful when it is computed within the virialization radius, which corresponds to the region where the cluster is expected to have reached dynamical equilibrium at the present epoch. The virialization radii, R_v , were computed in the same way as B95, i.e. by assuming a proportionality between the X-ray temperature and R_v^2 and by scaling to Coma values.

In Table 5 we list several quantities computed before and after the rejection of galaxies, which belong to the detected substructures: in Cols. (2) and (3) the global σ (in $km s^{-1}$); in Cols. (4) and (5) the virial mass as computed within the Abell radius (i.e. $1.5 h^{-1} Mpc$); in Col. (6) the virialization radius in $h^{-1} Mpc$; in Cols. (7) and (8) the virial mass as computed within the virialization radius.

The σ and mass distributions computed before and after removing substructures are not different according to the Kolmogorov-Smirnov test (see Press et al. 1992). This holds true both for masses and for σ computed within a fixed radius of $1.5 h^{-1} Mpc$ and within the virialization radius. As far as the individual values are concerned, only the mass of A85 shows a significant change. Indeed, as discussed in the appendix, its substructure is likely to be unbound and thus it may be only a chance superimposition on the cluster.

Our results are in agreement with E94 and partially in disagreement with B95, who found that the masses computed within the fixed radius depend on a possible correction for the presence of substructures. This is probably due to the fact that we consider as a *identified cluster*, in which we look for substructures, a sample detected by a more refined method than that used by B95, who employed a simple cut in velocity space within an Abell radius (Bird 1994). This fact could also explain why she detected substructures in clusters which we found were not substructured: the galaxies which belong to these substructures have probably been excluded in our procedure of identification of the cluster. Indeed, also B95 found no significant effect when the masses are computed within the virialization radius; in fact, this radius is generally smaller than

$1.5 h^{-1} Mpc$ and therefore the galaxy sample is naturally better cleaned.

Reassuringly, by considering the 16 unimodal clusters in common with B95, our distribution function of mass values does not significantly differ from that of B95's mass values corrected for substructures (column 10 in Table 1 of B95), according to the Kolmogorov-Smirnov test.

Our results do not disagree with Pinkney et al. (1996), who found, by considering simulations of a cluster with a merging clump (mass ratio 1:6 and 1:3), that the virial mass estimator overestimate the true cluster mass, in particular in the case of small projection angles of merger axis. In fact, our substructures are generally smaller (see Table 6) and the projection angles are likely greater. The most probable case of head-on merging, A85, actually shows a significant change in mass estimation.

Substructures can significantly affect small scale phenomena, e.g. the peculiarity of the cD galaxy velocities which depends on the removal of some substructures (see, e.g., A2063).

In Table 6 we list some interesting parameters for each substructure contained in unimodal clusters: in Col. (2), $N_{\%}$, the fraction of galaxies relative to the total of the galaxies contained within $1 h^{-1} Mpc$; in Col. (3), R , the maximum projected radius of the substructure computed by considering the biweight center (which is preferable to the density center when the number of galaxies is small, see Beers et al. 1990). The average values are $N_{\%} = 7.5\%$ and $R = 0.21 h^{-1} Mpc$.

The core structures detected do not appear to be a homogeneous class: they can contain few or many galaxies and can have a lower or higher σ than that of the whole cluster. The statistics is still too poor to draw general conclusions. However, they are so close in position and velocity to the respective cluster quantities, that we suspect they are cluster regions with a particular kinematical status (see e.g. A1795) or, if very extended, real virialized clusters (see e.g. A1185, A3391), rather than, e.g., the relics of some structures coming from the outside. Therefore, in the present analysis we do not consider samples obtained by rejecting the galaxies of core structures because it is probable that the remaining structures have no real physical significance.

TABLE 6

THE SUBSTRUCTURES

Cluster	$N_{\%}$	R
A0085S	8	0.19
A0193S	7	0.03
A0194S1	7	0.11
A0194S2	17	0.34
A1060S	6	0.04
A1367S	9	0.08
A1983S	9	0.22
A2063S	10	0.27
A2877S	8	0.10
A3667S	13	0.30

Nine of our clusters (A193, A194, A1631, A1795, A1809, A2063, A3128, A3558, A4038) show velocity dispersion profiles which decrease towards the cluster center. This behaviour may be due to the effect of dynamical friction, which slows down the most luminous, central galaxies with respect to the background matter (Merritt 1988), or to the loss of orbital energy during galaxy merging (Menci & Fusco-Femiano 1996). The same processes could explain the presence of core structures with a low- σ population which we find in four of the above clusters (A194, A1631, A1795, A3128) and in another cluster (A2877). The final consequence of these processes could be the formation of a cD galaxy. Nevertheless, only five of the above-mentioned clusters are cD clusters (A193, A1795, A1809, A2063, A3558) as expected in our sample, where about half of the clusters are cD clusters.

The above-mentioned behaviour of VDP as well as the core structures with a low velocity dispersion could be also explained by alternative scenarios. The velocity dispersion could increase with radius because of the inclusion of subclumps with different mean velocities or dispersions. However, some of the above clusters show no substructures in outer regions (e.g. A1631, A1795). In another scenario, the low dispersion population could be the remnants of a small subcluster, as suggested for the A576 cluster by Mohr et al. (1996).

The presence of a cooling flow and/or luminosity segregation, which are signs of possible relaxation, could allow us to distinguish whether the observed effects are due to dynamical relaxation or to the presence of substructures but, at present, the available information is poor. For instance, A1795 is well known to have a strong cooling flow, A2063 has a faint one, (Edge, Stewart, & Fabian 1992), as does A3558 (Bardelli et al. 1996), and A1809 has no cooling flow (Stewart et al. 1984). Biviano et al (1992) found evidence that luminous galaxies are segregated in velocity in A194, but they did not find any significant velocity segregation for A1631, A3128, A3558. Den Hartog & Katgert (1996) found faint evidence of luminosity segregation in A3128 and A3558 and no evidence in A194, A1631, A1809, and A2063.

5.4 Bimodal and Complex Clusters

As regards bimodal or complex clusters, the VDPs (see Figure 4 and Table 3) suggest that their internal kinematics strongly biases the estimate of σ .

TABLE 7

BIMODAL AND COMPLEX CLUSTERS

Cluster	Sample	Mass ($10^{14} M_{\odot}$)
(1)	(2)	(3)
A0548	MP	9.5 ± 0.9
	MS1+MS2	13.0 ± 1.3
	C+S1+S2+S3+MS2	9.5 ± 2.0
	C+MS2	6.4 ± 0.9
A0754	MS	1.7 ± 0.6
	MS1+MS2	2.5 ± 0.9
A2151	MS	6.0 ± 0.9
	S1+S2+S3	4.3 ± 1.7
A3526	MP	7.5 ± 0.9
	MS1+MS2	2.3 ± 0.5

In fact, these clusters could be cases of ongoing merging and their dynamical status may be rather far from virial equilibrium. In this respect, we stress the importance of using optical information, when one suspects a strong cluster merging and the presence of compression-heated gas (e.g. Zabludoff & Zaritsky 1995). In fact, the optical component seems much less disturbed by cluster collisions than the gas content, so that the galaxy systems could survive the first cluster encounter (McGlynn & Fabian 1984). In these cases the most meaningful mass estimate could thus be the sum of the virial masses of the (supposed virialized) clumps.

Table 7 shows, in Col. (3), the cluster masses computed both as the virial mass of the whole cluster and as the sum of virial masses of each subclump. Indeed, a precise mass estimate depends on the choice of the clumps considered (see, e.g. several mass estimates of A548). All these masses are computed within the respective virialization radii (§ 5.3), which are here computed by adopting σ rather than the X-ray temperature as an estimate of the potential depth. This choice is due to the fact that some systems are not clearly spatially identified in X-ray maps and that observed X-ray temperatures could not reliably measure the cluster potential well.

These two ways of computing the mass may give appreciably different results. In particular, in the case of the *head-on* bimodal cluster A3526, neglecting the presence of clumps in velocity space leads one to strongly overestimate the cluster mass. Indeed, by analyzing the two-clumps merging in simulated clusters, Pinkney et al. (1996) found that the cluster mass is strongly overestimated in the case of *head-on* two-clumps merging.

More accurate mass evaluations need the development of hydrodynamical simulations, which include a large range of initial parameters (e.g. angles of view and encounter velocities) and which describe both collisional and accollisional cluster components (e.g. Burns et al. 1995).

6 SUMMARY AND CONCLUSIONS

We analyzed a set of 48 galaxy clusters, which is the most extensive sample in the literature used to study the presence of substructures by means of galaxy positions and redshifts.

We used a multi-scale analysis which couples kinemat-

ical estimators with the wavelet transform (Escalera & Mazure 1992; Escalera et al. 1994), by introducing three new kinematical estimators. These estimators parameterize the departures of the local means and/or local dispersions of the measured radial velocities with respect to their global values for the environment.

Both the methods we apply for detecting substructures and for computing velocity means and dispersions (Beers et al. 1990) have the advantage of requiring no Gaussian velocity distributions. In fact, one expects non-Gaussian galaxy velocity distributions in clusters that, even in dynamical equilibrium, show the presence of velocity anisotropy in galaxy orbits (e.g. Merritt 1987).

We analyzed 44 cluster fields, recovering 48 clusters, of which 44 are detected with high significance (99.5%) and are sampled up to a sufficiently external region. Of the 44 clusters, we classify five clusters as bimodal, one as complex, and the others as unimodal. In 9 of the 38 unimodal clusters we clearly detect the presence of small-scale substructures and there is some sign of them in 12 others. Hence, we detect the presence of substructures in about one third of the clusters, in broad agreement with previous works which are based on different techniques. However, the high fraction of cD clusters in our sample (about 50%) suggests that our sample may be not strictly representative of the Universe. Indeed, this is the first part of a larger study planned to consider the other clusters specific to the ENACS database (Katgert et al. 1996) in order to obtain a more statistically significant sample.

To discuss the effect of substructures on cluster dynamics, one should consider that substructures can assume some basic forms (West & Bothun 1990).

The groups, which are not dynamically bound to the cluster, or bound units, which reside outside the relaxed portion of the cluster and are perhaps just falling in, are probably rejected in our phase of galaxy cluster identification, with the possible exception of A85.

The dynamical substructures that reside within an otherwise relaxed system may be the remnants of a previous secondary infall or cluster merging. The small-scale substructures we detected represent, on average, 7.5% of the cluster galaxies within $1 h^{-1} \text{ Mpc}$ and their average extension is $\sim 0.2 h^{-1} \text{ Mpc}$. The two values are in agreement with typical population fractions and sizes of substructures

inferred by small-scale correlations among galaxies observed in many apparently relaxed clusters (Salvador-Solé, González-Casado, & Solanes 1993; González-Casado, Solanes, & Salvador-Solé, 1993). The substructures we detect are probably sufficiently compact to survive the cluster force after merging, according to the theoretical work by González-Casado et al. (1994). These authors have suggested that these substructures could be the remnants of massive cores of groups or small clusters.

The effect of small substructures does not appear to be considerable on the global cluster kinematics and dynamics, i.e. on the value of the velocity dispersion and mass. This indicates that clusters which show only small substructures are not too far from dynamical equilibrium, as is also suggested by the generally good agreement between global X-ray and optical cluster properties (centers and velocity dispersions).

The above conclusions do not hold true for bimodal or complex clusters, which are likely cases of recent cluster merging.

From the point of view of statistical studies concerning galaxy clusters, the problem of the estimate of velocity dispersion and mass in bimodal and complex clusters might not be serious if their fraction is fairly small as in our sample. This could explain the result obtained by Biviano et al. (1993), who found no difference between the mass distribution of substructured and non-substructured clusters, and by Fadda et al. (1996), who found no difference in the cumulative distributions of cluster velocity dispersions whether or not they took into account the multimodality of some clusters in their velocity distributions.

We wish to thank the ENACS team for providing us with new data prior to publication. We thank the anonymous referee for useful remarks and comments. We are also indebted to Harald Ebeling, who gave us some X-ray data in advance of publication. We are grateful also to Vahe Gurzadyan for some enriching discussions on the philosophy of structure detection.

This work has been partially supported by the *Italian Ministry of University, Scientific Technological Research (MURST)*, by the *Italian Space Agency (ASI)*, and by the *Italian Research Council (CNR-GNA)*.

APPENDIX A RESULTS FOR INDIVIDUAL CLUSTERS.

We organize the presentation in the form of a series of paragraphs, each one corresponding to a cluster. For each cluster we describe the pure detection results obtained from our main procedure of systems identification. Moreover, by performing some particular analyses, as well by comparing our findings with the relevant results in the literature, we suggest the most probable dynamical status. It should be noted that it is not the purpose of this work to provide definitive conclusions regarding the dynamics of these clusters.

In the following discussions some notations are used.

The word *regular* means an almost symmetrical spatial shape combined with a Gaussian or nearly Gaussian velocity distribution.

To test whether two systems are unbound, we apply the two-body model (e.g. Beers, Geller & Huchra 1982), which gives both bound and unbound solutions by varying the value of the unknown projection angle between the two systems.

When no bound solutions are possible (Newton's criterion), we classify two structures as *unbound*.

A85. — Regular shaped cluster which contains a foreground group of 7 galaxies (S) in front of the center. No further substructure. The foreground group roughly corresponds to the one already shown by Malumuth et al. (1992) and Beers et al. (1991). Newton's criterion does not exclude the possibility that the S group may be bound. However, even if it is bound, it could be a sign of secondary infall to a pre-virialized cluster. Removing this group changes the σ (877_{-50}^{+61} $km\ s^{-1}$), which becomes lower than the σ expected from T , although still consistent at about two s.d.. Moreover, the cleaned cluster shows an acceptably Gaussian velocity distribution.

A119. — Regular shaped cluster. From inspection of X-ray maps and galaxy isopleths derived from photometry, Fabricant et al. (1993) suggested the presence of multiple structures. Although the number of galaxy redshifts is now almost doubled, the cluster kinematics does not show any evidence of substructures. This is not, however, a clear contradiction of the suggestion of Fabricant et al. (1993), since their supposed configuration is beyond the limits of our detection method (see §3.1). The only possible evidence of substructures is the disagreement between σ and T (at about 2.5 s.d.).

A151. — Two distinct populations in terms of velocity (MS1,MS2), separated by almost 4000 Km/s, slightly overlapping but easy to identify. These two populations correspond to those already identified by Proust et al. (1992): the real cluster and a foreground group, respectively. We confirm that these systems are unbound according to Newton's criterion.

A193. — Regular cluster. However, a close quartet close to the center appears significant (S). The VDP shows a strong decrease towards the cluster center, which suggests a possible advanced dynamical status (see the discussion in § 5.3), confirmed also by the presence of a cD galaxy.

A194. — Two loose background groups (US1,US2), gravitationally unbound to the cluster. Significant small-scales structures are present within the cluster: a triplet (S1), a close septet (S2) and a very condensed core (C). In this case the identification of the main system within the main peak produces macroscopic results. The cluster becomes regular and the VDP becomes flat in the external region as expected in a cluster which is in a state of dynamical equilibrium. The core has a low velocity dispersion. By subtracting the core structure, the σ of the cluster increases by about 100 $km\ s^{-1}$, approaching the observed value of the X-ray temperature.

A262. — True cluster, poorly populated after removing loose disperse galaxies of the field, whose presence is due to the fact that this cluster belongs to the Perseus supercluster.

A399-401. — Bimodal system, the two populations (MS1=A401, MS2=A399) slightly overlapping but separated in velocity by almost 700 $km\ s^{-1}$. No further substructures. The separation of A399 and A401 is considerably difficult because the clusters are fairly close together in radial velocity (see e.g. Oegerle & Hill 1994; Girardi et al. 1996). The two-body model confirms that these two clusters are probably gravitationally bound (see also Oegerle & Hill 1994). Some evidence that A401 is a multiple cluster comes from Slezak et al. (1994). Recent results by Fujita et al. (1996), based on X-ray data, suggest that these clusters are really interacting but that the interaction is not strong at present; however, they cannot exclude the possibility that there was a past first encounter. As a possible sign of a substructure, we find that the cD galaxy in A401 cluster has a relevant peculiar velocity.

A426. — Initially extended field. The main cluster (MS) shows an irregular (elongated) shape and a regular velocity distribution. There is a strong clustering (C) in the central region. The C structure appears rather dynamically perturbed (i.e. with a high dispersion), although its mean velocity well agrees with that of the cluster. Indeed, it has been recently claimed that this cluster does not appear to be in a complete relaxed state. In particular, Mohr, Fabricant, & Geller (1993) found substructures in the core. Also Slezak et al. (1994) found a double peak in the core by analyzing X-ray data: however, the region they analyzed is smaller than our minimum scale analyzed. This cluster is well-known for showing a β -problem ($\beta = 1.78_{-0.34}^{+0.48}$ in Edge & Stewart 1991b). The σ is now in acceptable agreement with the estimate of T ($\beta = 1.25_{-0.22}^{+0.24}$). Other observational evidence for reducing the value of σ comes also from Fadda et al. (1996, $\beta = 1.01_{-0.16}^{+0.24}$). The strong increase in the VDP towards the cluster center suggests the presence of galaxies with radial orbits in the external cluster region, as already suggested by, e.g., Solanes & Salvador-Solé (1990). The acceptable agreement between σ and T suggest that these galaxies, although recently infalled into the cluster, are already roughly virialized within the cluster potential.

A539. — Two systems (MS1, MS2), both very extended, separated in velocity by over 4000 Km/s, but spatially overlapped. MS1, whose condensed core should be the real structure, has to be considered a foreground group (see also Pisani 1993). Cluster A539 should be the condensed core of the MS2 clump. In order to better analyze the cluster we considered the whole published data sample within 6 $h^{-1} Mpc$ from the X-ray center of the cluster (A539*). This sample is not nominally complete; however, we can probably rely on some uniformity in a small region, e.g. the region close to the cluster center, where substructures are detected. At the intermediate scale we detected a core structure C, which contains two structures (C1, C2) at the small scale. The C1 clump corresponds to the core of the above detected MS2, while the C2 clump is at higher redshift.

A548. — The very irregular velocity distribution suggests a complex dynamical status (see e.g. Davis et al. 1995). The

optical data clearly show a bimodal aspect with two systems, MS1 and MS2, which correspond respectively to the SW and NE X-ray components (i.e. S2 and S1 in Davis et al., 1995). Within the MS1 component we detect 3 substructures (S1,S2,S3) and a core structure (C), which well corresponds to the X-ray center. Also Davis et al. (1995), by using partially different redshift data, found that the SW optical region is complex. The σ of the MS2 sample well agrees with the respective estimate of T . On the contrary, the T of the other component differs (but not significantly within the errors) by about 200 km s^{-1} from the σ of MS1, but well agrees with the σ of its core. This suggests that the core is the virialized part of the SW component and is responsible for the observed X-ray emission. The surrounding galaxies and clumps may not yet be in dynamical equilibrium. More precise T estimates could easily solve this problem.

A754. — The MS sample is elongated and includes two lobes, while US is an external structure. At the intermediate scale, we detected the MS1 (NW) and the MS2 (SE) lobes; C is a core structure detected in MS2 and represents half of the lobe. D88 did not detect any significant substructure, but bimodality is displayed in recent X-ray and optical data (e.g. Zabludoff & Zaritsky 1995). In the VDP (see Figure 4) we used the galaxy density centers rather than the X-ray one. In fact, optical structures do not correspond to the X-ray ones in this cluster, which shows direct evidence of an on-going collision (see Henry & Briel 1995; Zabludoff & Zaritsky 1995; Heriksen & Markevitch 1996).

A1060. — Almost regular cluster with a dynamically perturbed condensed core (C) and a close quintet at South (S1). The core structure appears better defined by using the less complete sample (A1060*) whose completeness level is only 50%. In this second sample the core structure represents an important fraction of the total population of the cluster. Although this cluster appears very regular, several authors have suggested the presence of substructures. For instance, Fitchett & Webster (1987) pointed out that their σ value is too high to agree with the value expected from X-ray luminosity. Indeed, our σ , which is similar to their value, is too low with respect to the X-ray temperature. The apparent discrepancy is explained by the fact that this cluster does not fit the usual relation between luminosity and temperature (e.g. David et al. 1993). This finding could suggest some anomalies in the dynamical status of the gas, rather than in that of the galaxies.

A1146. — Distant and regular cluster. The agreement with T is sufficiently good if we consider that this T is not measured but only estimated from X-ray luminosity.

A1185. — The field usually attributed to A1185 does not refer to the cluster itself, since it includes a large and uniform environment. The true cluster could consist in the condensed structure in the center (C). Already Fadda et al. (1996) noted the anomalous increase of the VDP in the external region of the cluster and naively suggested neglecting this region.

A1367. — This cluster belongs to the Coma supercluster. Irregular in shape and velocity distribution, this cluster contains a close sextet (S).

A1631. — Very irregular in shape despite a regular velocity distribution. This cluster shows a very elongated structure (C), which passes through the cluster center and contains some bright galaxies. This anomalous shape could suggest that the real core structure might be C1, which is a close significant sextet included in C. These central structures were not detected by D88. Moreover, the substructures found by E94, who analyzed the same galaxy sample, are not detected in this work; this discrepancy with E94 is discussed in § 3.1.

A1644. — Regular cluster. The velocity distribution shows a secondary peak which corresponds to an extended foreground structure ($\Delta V = 1100 \text{ Km/s}$). Both populations are fully overlapping with each other and cannot be separated; no significant US structure is identified. We use the same galaxy sample as Dressler & Schechtman (1988b), who found that the presence of substructures in this cluster is not definitively significant (c.l. about 97%). E94 found substructures which are not shown here. However, the peculiar velocity of the cD galaxy suggests the possible presence of a minor substructure.

A1736. — Cluster A1736 shows two well separated peaks in the velocity distribution. The main peak corresponds to A1736B, according to the denomination by D88. We do not analyze the foreground peak (A1736A) because of the small number of objects. By analyzing the same data sample, D88 found substructures, which are significant only at about 98%. Fadda et al. (1996) found two peaks in the velocity distribution, but so strongly overlapping with each other that their physical separation was uncertain. According to our analysis, A1736B does not show substructures and this finding is confirmed by the good agreement with T .

A1795. — Regular cluster with a central condensation (C). Hill & Oegerle (1993) detected substructures significant only at about 97%. The VDP of the main sample strongly decreases towards the cluster center. The low- σ core structure C contains a cD galaxy, whose velocity is consistent with the mean velocity of the C structure and that of the whole cluster. Moreover, a strong cooling flow was observed (Edge et al. 1992; Cardiel, Gorgas & Aragon-Salamanca 1995). All these findings indicate that this cluster is a very relaxed cluster (see also the discussion in § 5.3). The better agreement of T with the σ of the MS-C sample rather than with the MS sample could confirm that the galaxies in the core could have been slowed down by relaxation processes (e.g. dynamical friction).

A1809. — Poor cluster, no substructures. Oegerle & Hill (1994) found no presence of substructures either. The VDP referred to the X-ray center is very noisy in the center; thus we prefer to show the VDP referred to the galaxy density center, which shows a clear decrease towards the central region.

A1983. — This cluster is characterized by an asymmetric velocity distribution, but this irregularity vanishes after

removing a significant foreground quintet located close to the center (S). The situation is similar to that found in A85, where the S could be an unbound foreground group, but in this case the S substructure causes a less significant variation of the total σ . D88 found the presence of substructures only significant at about 94%. E94 found a substructure both in the center and in the cluster field, but none associated with the S detected in this work.

A2052. — Irregular cluster, contains some disturbing objects (pairs, triplets) which, however, do not constitute any significant substructure. Malumuth et al. (1992) found no significant structure, either. The global σ is lower than T , but agrees within two s.d..

A2063. — This field contains two clusters that are very distant from each other in terms of velocity ($\Delta V \sim 3000$ Km/s): MS1 and MS2, which correspond to A2063 and MKW3S, respectively. The MS1 sample contains a substructure of seven very close galaxies (S), largely background. However, according to the Newton criterion, we cannot exclude the possibility that S is bound to the remaining galaxies in the MS1 sample. For the same reason we cannot rule out the possibility that MS1 and MS2 samples may be bound. Both clusters contain cD galaxies; however, the cD galaxy of A2063 has a peculiar velocity: this peculiarity disappears when we reject its substructure S.

A2107. — Remarkably regular cluster. Oegerle & Hill (1992) found evidence of substructures by using the test of D88. The peculiar velocity of the cD galaxy could suggest a situation of non-perfect dynamical equilibrium. However, with the present data, there is good agreement between σ and T .

A2124. — Regular cluster.

A2151. — Highly structured cluster, despite an apparently regular velocity distribution of the main field. We notice a significant central structure C ($\Delta V \sim -700$ km s⁻¹), an extended subsystem S1 at North and a close background quintet S2 at East. These three subsystems, very distant from each other, concern about 50% of the total population of the cluster. These results are consistent with E94. Bird, Davis, & Beers (1995) find that X-ray and optical distributions are not very similar. We confirm this result: in particular, our central C is not centered on the X-ray cluster center. This fact and the large velocity of C with respect to that of the whole cluster suggest that C could be considered a real substructure rather than a particularly relaxed central region. This cluster should be regarded as a case of present cluster merging. Moreover, although the σ of the MS sample is in good agreement with the T by David et al. (1993), it is higher than the T s detected by Bird et al. (1995) for the individual clumps.

A2197-2199. — No significant structures, thought elongated in shape. The field we analyzed contains, however, the two well-known clusters A2197 and A2199, which correspond closely to the structures we detect at a very low significance level (about 60%). The background system MS1 in the South (A2199) contains a close foreground quartet (S1), while the foreground system MS2 at North (A2197) contains a background quartet (S2). This peculiar situation is very difficult to analyze with our method, since the local kinematics cannot be cleaned from the mutual contamination produced by the four systems. Therefore, we do not consider these clusters in the final discussion.

A2634-2666. — The MS sample includes both A2634 and the tiny cluster A2666 (S1) and a further substructure (S2). We identify A2634 with the MS-S1-S2 sample, i.e. the MS sample after the rejection of A2666 and S2, which are both unbound to the remaining galaxies. The “identified cluster” main properties are: Center 1950 (α, δ)=233606.9+264541; $N=216$; $R_{max}=5.64$; $\bar{v} = 9136$ km s⁻¹; $P_W < 0.1\%$; $\sigma=886$. Scodreggio et al. (1995) did not find any evidence of substructures in the central cluster region. The σ of the MS-S1-S2 sample is in good agreement with the T at about 1 h^{-1} Mpc, and an increase in the outer region is likely because of the presence of some remaining interlopers. The T of A2666 is much higher than our value of σ , but we note that this T is estimated from X-ray luminosity.

A2670. — We analyze two samples. A2670, the first sample, does not contain any substructures. The second sample A2670*, which is deeper and has a smaller extension, contains a foreground group of galaxies (US) at West of the main system. Sharples et al. (1988) did not find any firm statistical evidence of subclustering, either. On the contrary, E94 found a series of structures which are not present in this analysis. B95, by taking into account the presence of substructures, reduces the peculiar velocity of cD. Here we still found a peculiar velocity for the cD galaxy, but this peculiarity disappears when we consider the deepest sample A2670*.

A2717. — This cluster contains a significant core structure (CS), slightly foregrounded ($\Delta V \sim -600$ km s⁻¹), which involves about 40% of the whole population and contains the cD galaxy. This feature is responsible for the asymmetry observed in the velocity distribution. The cD galaxy, which has not a peculiar velocity with respect to the MS sample but only with respect to the C structure, confirms that this core is probably dynamically perturbed.

A2721. — Regular cluster. We show the VDP referred to the galaxy density center, which is more regular than that computed with the X-ray center.

A2877. — Regular velocity distribution, irregular shape. We detect two significant subsystems: the core structure (C), and a structure (S) at North.

A3128. — The analyzed field contains an extended structure at South (US), which gives the cluster its elongated shape. The main cluster MS is regular, with a very condensed structure in the center (C). We report the VDP computed with the galaxy density center, which is more regular than that referred to the X-ray center.

A3266. — The analyzed field contains two systems, which are very similar in terms of velocity but spatially far apart. The smallest group is elongated (US) and lies at East of the main dominant system (MS). This one is regular and should

correspond to the real cluster. The VDP of MS is very noisy in the central region and the σ is higher than the T , but consistent within two s.d..

A3376. — Regular velocity distribution despite its irregular shape. The central region appears elongated. The South part of this group appears well coincident with the X-ray center; thus we prefer to denominate it a core structure, although it is probable that its North component may be a real substructure. D88 found substructures less significant than 95%. The substructures detected by E94 are not present in this analysis (see § 3.1).

A3391-3395. — Rich field with two distinct clusters, partially overlapping, but well separated in velocity. The dominant system (MS1=A3395) is a rich extended cluster, which has a regular velocity distribution but is almost irregular in shape. The small scale analysis reveals a significant central condensation (C1), which is elongated and dynamically similar to the main system. A small system at North (MS2=A3391), in the background of MS1 ($\Delta V \sim 2000 \text{ km s}^{-1}$), is formed by a core structure (C2) appended to some loose background galaxies. Girardi et al. (1996) pointed out the difficulty in separating the two clusters and used the VDP to truncate the clusters at the radius, where the VDP increases owing to the presence of a close cluster. The present method is able to separate the clusters and gives VDPs, which are flat in the external region. The cD galaxy of A3391 has a peculiar velocity with respect to MS2, but not with respect to C2, which contains the cD galaxy.

A3526. — We analyzed two samples (A3526 and A3526*), the former deeper in magnitude and with a minor extension than the latter. In both samples we identify two dominant significant systems (MS1, MS2). They are fairly well separated in velocity ($\Delta V \sim 1500 \text{ km s}^{-1}$), but fully overlapped and probably bound. MS2 contains a condensed structure at East (C), whose center corresponds to its galaxy density center. In the sample A3526*, MS1 includes a group of foreground galaxies (S), which is probably unbound ($\Delta V = -1000 \text{ km s}^{-1}$). The velocity distribution of MS1 becomes regular if we exclude S.

Already Lucey, Currie, & Dickens (1986) detected the presence of two peaks in the velocity distribution and found that only a minority of the galaxies (30%) in the secondary peak in the cluster A3526 could actually be distant from the primary peak. The cluster should be thus regarded as a strongly substructured cluster (see also Mohr et al. 1993). Girardi et al. (1996) and Fadda et al. (1996) indicated this cluster as one with a problematic dynamics by using the velocity distribution. A likely on-going merging might explain the high temperature of the collision-heated gas.

Shapley region. — The analyzed field contains two well sampled main clusters: A3558 and A3562. MS is the dominant group, which contains the cluster A3558. US1 is a small group at West, clearly separated in position on the basis of the available data. US2 is a large group at East, slightly foregrounded with respect to US1. Both US1 and US2 have a high dispersion because they probably do not correspond to true physical systems. In fact, US2 contains a structure (US2S), which is significant at the 80% c.l. and correspond to A3562. Due to the limited value of significance, we do not consider this cluster in the final discussion, although the good agreement with T suggests a good real identification. MS is a rich and very structured system despite its regular velocity distribution. The analysis at small scales reveals three distinct groups inside: a background structure S1 at North ($+800 \text{ km s}^{-1}$); a very condensed structure at East S2, which also contains the poor cluster SC1329-314; a central structure S3, which is dynamically similar to the main system and corresponds to the identified A3558 cluster.

The internal structure of A3558 is widely debated in the literature and the T of this cluster is well known to be lower than σ (see e.g. by Bardelli et al. 1996, who report $\beta = 1.79$). Our S3 structure, which we identify as A3558, has a σ compatible with T ($\beta = 0.86^{+0.39}_{-0.23}$), although the peculiar velocity of the cD galaxy may suggest the presence of internal substructures.

A3667. — Asymmetric and dynamically regular cluster, although it includes a significant, very condensed structure S, which is remarkably elongated. No further substructures appear significant. The global σ s of MS or MS-C samples are in good agreement with T , although the VDP is very noisy in the central cluster region.

A3716. — Cluster A3716 is clearly divided into North and South components (D88). Hence, this cluster is an apparent case of large-scale structure. The MS we detect is the richest South component, since the data of North component are too scarce. This South component is an apparently regular structure. We adopt the optical center for the computation of the VDP, since it is more regular towards the center than the VDP referred to the X-ray center.

A3888. — Almost regular cluster but with an asymmetric velocity distribution. The local dispersions are atypically high due to the presence of numerous field galaxies uniformly distributed through the whole extension of the cluster, thus suggesting a systematic contamination effect.

A4038. — Regular cluster. Unfortunately, the region of this cluster we studied is too small to permit a good check of the VDP. The VDP centered on the optical center is less noisy than that centered on the X-ray center, but we cannot be sure that the VDP remains flat towards the external cluster regions.

REFERENCES

- Abramopoulos, F., & Ku, W. H. M. 1983, *ApJ*, 271, 446
- Bahcall, N. A. 1977, *ApJ*, 217, L77
- Bahcall, N. A., & Cen, R. 1993, *ApJ*, 408, L77
- Bardelli, S., Zucca, E., Vettolani, G., Zamorani, G., Scaramella, R., Collins, C. A., & MacGillivray, H. T. 1994, *MNRAS*, 267, 665
- Bardelli, S., Zucca, E., Malizia, A., Zamorani, G., Scaramella, R., & Vettolani, G. 1996, *A&A*, 305, 435
- Beers, T. C., Flynn, K., & Gebhardt, K. 1990, *AJ*, 100, 32
- Beers, T. C., Forman, W., Huchra, J. P., Jones, C., Gebhardt, K. 1991, *AJ*, 102, 1581
- Beers, T. C., Geller, M. J., & Huchra, J. P. 1982, *ApJ*, 257, 23
- Beers, T. C., Forman, W., Huchra, J. P., Jones, C., & Gebhardt, K. 1991, *AJ*, 102, 1581
- Beers, T. C., & Tonry, J. L. 1985, *ApJ*, 300, 55
- Beers, T. C., & Tonry, J. L. 1986, *ApJ*, 300, 557
- Bird, C. M. 1994, *ApJ*, 422, 480
- Bird, C. M. 1995, *ApJ*, 445, L81, (B95)
- Bird, C. M., & Beers T. C. 1993, *AJ*, 105, 1586
- Bird, C. M., Davis, D. S., & Beers T. C. 1995, *AJ*, 109, 920
- Biviano A., Durret, F., Gerbal, D., Lefèvre, O., Lobo, C., Mazure, A., & Slezak, E. 1996, *A&A*, in press
- Biviano, A., Girardi, M., Giuricin, G., Mardirossian, F., & Mezzetti, M. 1992, *ApJ*, 396, 35
- Biviano, A., Girardi, M., Giuricin, G., Mardirossian, F., & Mezzetti, M. 1993, *ApJ*, 411, L13
- Briel U. G., & Henry P. J. 1994, *Nature*, 372, 439
- Bothun, G. D., & Schombert, J. M. 1988, *ApJ*, 335, 617
- Breen, J., Raychaudhury, S., Forman, W., & Jones C. 1994, *ApJ*, 424, 59
- Burns, J. O., Rhee, G., Owen, F. N., Pinkney, J. 1994, *ApJ*, 423, 94
- Burns, J. O., Roettiger, K., Pinkney, J., Perley, R. A., Owen, F. N., & Voges, W. 1995, *ApJ*, 446, 583
- Butcher, H. R., & Oemler, A. Jr. 1985, *ApJS*, 57, 665
- Cardiel, N., Gorgas, J., & Aragon-Salamanca, A. 1995, *MNRAS*, 277, 502
- Chapman, G. N. F., Geller, M. J., & Huchra, J. P. 1988, *AJ*, 95, 999
- Colless, M., & Hewett P. 1987, *MNRAS*, 224, 453
- Colless, M. 1989, *MNRAS*, 237, 799
- David, L. P., Slyz, A., Jones, C., Forman, W., Wrtilek, S. D., & Arnaud, K. A. 1993, *ApJ*, 412, 479
- Davis, D. S., Bird, C., Mushotzky, R. F., & Odewahn, S. C. 1995, *ApJ*, 440, 48
- den Hartog, R., & Katgert, P. 1996, *MNRAS*, 279, 349
- Dickens, R. J., Currie, M. J., & Lucey, J. R. 1986, *MNRAS*, 220, 679.
- Dickens, R. J., & Moss, C. 1976, *MNRAS*, 174, 47.
- Dressler, A. 1980, *ApJS*, 42, 565.
- Dressler, A., & Shectman, S. A. 1988a, *AJ*, 95, 284
- Dressler, A., & Shectman, S. A. 1988b, *AJ*, 95, 985 (D88)
- Ebeling, H., Voges, W., Boehringer, H., Edge, A. C., Huchra, J. P., Briel, U. G. 1996, *MNRAS*, 281, 799
- Edge, A. C., & Stewart, G. C. 1991a, *MNRAS*, 252, 414
- Edge, A. C., & Stewart, G. C. 1991b, *MNRAS*, 252, 428
- Edge, A. C., Stewart, G. C., & Fabian 1992, *MNRAS*, 258, 177
- Elvis, M., Plummer, D., Schachter, J., & Fabbiano, G. 1992, *ApJS*, 80, 257
- Escalera, E., & Mazure, A. 1992, *ApJ*, 388, 23
- Escalera, E., Biviano, A., Girardi, M., Giuricin, G., Mardirossian, F., Mazure, A., & Mezzetti, M. 1994, *AJ*, 423, 539 (E94)
- Escalera, E., & MacGillivray, H. T. 1995, *A&A*, 298, 1
- Ettori, S., Guzzo, L., & Tarengchi, M. 1995, *MNRAS*, 276, 689
- Evrard, A. 1990, *ApJ*, 363, 349
- Fabricant, D., Kurtz, M., Geller, M., Zabludoff, A., Mack, P., & Wegner, G. 1993, *AJ*, 105, 788
- Fadda, D., Girardi, M., Giuricin, G., Mardirossian, F., & Mezzetti, M. 1996, *ApJ*, 473, 670
- Fitchett, M. J. 1988, in *The Minnesota Lectures on Clusters of Galaxies and Large-Scale Structures*, ed. J. M. Dickey (ASP Conf. Ser., 5), 143
- Fitchett, M. J., Webster, R. L. 1987, *ApJ*, 317, 653
- Fujita, Y., Koyama, K., Tsuru, T., & Matsumoto, H. 1996, *PASJ*, in press (preprint astro-ph/9602059)
- Gavazzi, G. 1987, *ApJ*, 320, 96
- Gebhardt, K., & Beers, T. C. 1991, *ApJ*, 383, 72
- Geller, M. J., & Beers, T. C. 1982, *PASP*, 94, 421
- Giovannelli, R., Haynes, M. P., & Chincarini, G. L. 1982, *ApJ*, 262, 442
- Girardi, M., Fadda, D., Giuricin, G., Mardirossian, F., Mezzetti, M., & Biviano, A. 1996, *ApJ*, 457, 61
- Giuricin, G., Mardirossian, F., & Mezzetti, M. 1982, *ApJ*, 255, 361
- González-Casado, G., Solanes, J. M., & Salvador-Solé, E. 1993, *ApJ*, 410, 15
- González-Casado, G., Mamon, G., Salvador-Solé, E. 1994, *ApJ*, 433, L61
- Grebenev, S. A., Forman, W., Jones, C. & Murray, S. 1995, *ApJ*, 445, 607
- Gregory, S. A., & Thompson, L. A. 1978, *ApJ*, 222, 784
- Gregory, S. A., & Thompson, L. A. 1984, *ApJ*, 286, 422
- Gregory, S. A., Thompson, L. A., & Tift, W. G. 1981, *ApJ*, 243, 411
- Gurzadyan, V. G., Harutyunyan, V. V., Kocharyan, A. A. 1994, *A&A*, 281, 964
- Gurzadyan, V. G., & Mazure, A. 1996, in preparation
- Henriksen, M. J. 1992, *AJ*, 103, 1051
- Henriksen, M. J., & Markevitch, M. 1996, *ApJ*, submitted (preprint astro-ph/9604150)
- Henry, J. P., & Briel, U. G. 1995, *ApJ*, 443, L9
- Heisler, J., Tremaine, S., & Bahcall, J. N. 1985, *ApJ*, 298, 8
- Hill, J. M., et al. 1988, *ApJ*, 332, L23
- Hill, J. M., & Oegerle, W. R. 1993, *AJ*, 106, 831
- Hintzen, P. 1980, *AJ*, 85, 626
- Ikebe, Y. et al. 1994, *ASCA preprint*
- Jones, C., & Forman, W. 1984, *ApJ*, 276, 38
- Jones, C., & Forman, W. 1992, in *Clusters and Superclusters of Galaxies*, ed. A. C. Fabian (Dordrecht: Kluwer), p. 49
- Katgert, P., et al. 1996, *A&A*, 310, 8
- Kent, S. M., & Sargent, W. L. W. 1983, *AJ*, 88, 697
- Lacey, C. G. & Cole, S. 1993, *MNRAS*, 262, 627
- Lauberts, A., Valentijn, E. A. 1989, "The Surface Photometry Catalogue of the ESO-Uppsala Galaxies", Garching bei Muenchen: ESO
- Lucey, J. R., Currie, M. J., & Dickens, R. J. 1986, *MNRAS*, 211, 453
- Lucey, J. R., & Carter, D. 1988, *MNRAS*, 235, 1177
- Malumuth, E. M., Kriss, G. A., Van Dyke Dixon, W., Ferguson, H. C., & Ritchie, C. 1992, *AJ*, 104, 495
- Mazure, A., et al. 1996, *A&A*, 310, 31
- McGlynn, T. A., & Fabian, A. C. 1984, *MNRAS*, 208, 709
- McHardy, I. M., Lawrence, A., Pye, J. P., Pounds, K. A. 1981, *MNRAS*, 197, 893
- McMillan, S. L. W., Kowalsky, M. P., & Ulmer, M. P. 1989, *ApJS*, 70, 723
- Menci, N., Fusco-Femiano, R. 1996, *ApJ*, in press
- Merrifield, M. R., & Kent, S. M. 1991, *AJ*, 101, 783
- Merritt, D. 1987, *ApJ*, 313, 121.
- Merritt, D. 1988, in *The Minnesota Lectures on Clusters of Galaxies and Large-Scale Structures*, ed. J. M. Dickey (ASP Conf. Ser., 5), p. 175
- Metcalf, N., Godwin, J. G., & Spenser, S. D. 1987, *MNRAS*, 225, 581
- Mohr, J. J., Fabricant, D. G., & Geller, M. J. 1993, *ApJ*, 413, 492
- Mohr, J. J., Geller, M. J., Fabricant, D. G., Wegner, G., Thorstein, J., & Richstone, D. O. 1996 accepted in *ApJ* (preprint astro-ph/9604169)
- Moss, C., & Dickens, R. J. 1977, *MNRAS*, 178, 701
- Nilson, P. 1973, *Uppsala General Catalogue of Galaxies*, Almqvist and Wiksell, Stockholm
- Oegerle, W. R., & Hill, J. M. 1992, *AJ*, 104, 2078
- Oegerle, W. R., & Hill, J. M. 1994, *AJ*, 107, 857
- Ostriker, E. C., Huchra, J. P., Geller, M. J., & Kurtz, M. J. 1988, *AJ*, 96, 1775
- Pierre, M., Bohringer, H., Ebeling, H., Voges, W., Schuecker, P., Cruddace, R., & MacGillivray H. 1994, *A&A*, 290, 725
- Piro, L., & Fusco-Femiano, R. 1988, *A&A*, 205, 26

- Pisani, A. 1993, MNRAS, 265, 706
- Pinkney, J., Rhee, G., & Burns, J. O. 1993, ApJ, 416, 36
- Pinkney, J., Roettiger, K., Burns, J. O., & Bird, C. A. 1996, ApJS, 104, 1
- Press, W. H., Teukolsky, S. A., Vetterling, W. T., & Flannery, B. P. 1992, Numerical Recipes (2d ed.; Cambridge: Cambridge Univ. Press)
- Proust, D., Quintana, H., Mazure, A., da Souza, R., Escalera, E., Sodré, L. Jr., & Capelato, H. V. 1992, A&A, 258, 243
- Quintana, H., Melnick, J., Infante, L., & Thomas, B. 1985, AJ, 90, 410
- Rhee, J. F. R. N., & Latour, H. J. 1991, A&A, 243, 338
- Richter, O.G. 1987, A&AS, 67, 237
- Richter, O.G. 1989, A&AS, 77, 237
- Roettiger, K., Burns, J., & Locken, C. 1993, ApJ, 413, 492
- Sarazin, C. L. 1986, Rev. Mod. Phys., 58, 1
- Salvador-Solé, E., González-Casado, G., & Solanes, J. M. 1993, ApJ, 410, 1
- Schindler, C. L. & Boehringer, H. 1993, A&A, 269, 83
- Schindler, C. L. & Mueller, E. 1993, A&A, 272, 137
- Scodeggio, M., Solanes, J. M., Giovanelli, R., Haynes, M. P. 1995, ApJ, 444, 41.
- Sharples, R. M., Ellis, R. S., & Gray, P. M. 1988, MNRAS, 231, 479
- Shapiro, S. S., & Wilk, M. B. 1965, Biometrika, 52, 591
- Slezak, E., Bijaoui, A., Mars, G. 1990, A&A, 227, 301
- Slezak, E., Durret, F., Gerbal, D. 1994, AJ, 108, 1996
- Sodre', L., Capelato, H. V., Steiner, J. E., Proust, D., & Mazure, A. 1992, MNRAS, 259, 233
- Solanes, J. M., & Salvador-Solé, E. 1990, A&A, 234, 93
- Soltan, A., Henry, J. P. 1983, ApJ, 271, 442
- Stewart, G. C., Fabian, A. C., Jones, C., & Forman, W. 1984, ApJ, 285, 1
- Struble, M. F., & Ftaclas, C., AJ1994, 108, 1
- Struble, M. F., & Rood, H. J. 1987, ApJS, 63, 555
- Teague, P. F., Carter, D., & Gray, P. M. 1990, ApJS, 72, 715
- The, L. S., & White, S. D. M. 1986, AJ, 92, 1248
- Tift, W. G. 1978, ApJ, 222, 54
- Tormen, G., Bouchet, F. R., & White, S. D. M. 1996, MNRASsubmitted (preprint astro-ph/9603132)
- Ueda H., Makoto I., Yasushi S. 1993, ApJ, 408, 3
- West, M. J. 1994, in Clusters of Galaxies, eds. F.Durret, A.Mazure, and J.Tran Thanh Van,, p.23
- White, D. A., & Fabian, A. C. 1995, MNRAS, 273, 72
- Yamashita, K. 1992, in Frontieres of X-ray Astronomy (Tokyo: publisher unknown), 473
- Zabludoff, A. I., Franx M., & Geller, M. J. 1993, ApJ, 419, 47
- Zabludoff, A. I., Geller, M. J., Huchra, J. P., & Vogeley, M. S. 1993, AJ, 106, 1273
- Zabludoff, A. I. & Zaritsky, D. 1995, ApJ, 447, L21
- Zwicky, F., Herzog, E., Wild, P., Karpowicz, M., & Kowal, C. 1961 - 1968, Catalog of Galaxies and of Clusters of Galaxies, vol.s 1-6 (Pasadena: California Institute of Technology)